Revision 2

Oceanic lavas sampling the high $^{3}He/^{4}He$ mantle reservoir: Primitive, depleted, or re-enriched?

G. Garapić[a,1], A. Mallik[b], R. Dasgupta[b], M.G. Jackson[a]

[a]Department of Earth Science, University of California, Santa Barbara, CA, USA

[b]Department of Earth Science, Rice University, Houston, TX, USA

[1]Corresponding author; email address: garapicg@newpaltz.edu; Presently at the Geology Department, SUNY New Paltz, New Paltz, NY, USA

Abstract

Helium isotopes are used as a tracer for primitive reservoirs that have persisted in the Earth's mantle. Basalts erupted at several intraplate oceanic islands, including Hawaii, Iceland, Galapagos and Samoa, have hosted the highest $^{3}He/^{4}He$ ratios (> 30 Ra, where Ra is atmospheric $^{3}He/^{4}He$ ratio) globally that are far in excess of the $^{3}He/^{4}He$ typical of the upper mantle sampled at mid-ocean ridges (8 Ra). These lavas have been suggested to be melts of a primitive, or possibly slightly depleted, mantle reservoir, i.e., either fertile or a depleted peridotite. Here we report evidence for geochemical enrichment in the high $^{3}He/^{4}He$ mantle sampled by lavas with the highest $^{3}He/^{4}He$ from Hawaii, Samoa and possibly Galapagos. The titanium concentrations in high $^{3}He/^{4}He$ lavas from Samoa are too high to be explained by melts of a mantle peridotite, even at infinitesimally small degrees of melting, and the elevated Ti corresponds to elevated Pb-isotopic ratios. The highest $^{3}He/^{4}He$ lavas from Loihi, Hawaii also have Ti concentrations that are too high to be melts of primitive mantle peridotite at the degrees of melt extraction proposed for this ocean island. Thus, Ti-rich material must have been added to the high $^{3}He/^{4}He$ mantle reservoir, and this material is likely to be recycled mafic crust similar to MORB-like eclogite, which is consistent with the elevated Pb-isotopic ratios. We show that fractionation corrected, major element compositions of high $^{3}He/^{4}He$ alkalic lavas can be satisfactorily modeled by melting and melt-rock interaction scenario in a fertile

peridotite-MORB-eclogite hybrid system. Primitive peridotitic and recycled eclogitic reservoirs are suggested to be intimately associated in the deepest mantle and high $^{3}He/^{4}He$ lavas from several localities may sample a mantle source that hosts a component of recycled oceanic crust.

Keywords:

intraplate volcanism, ocean island basalts, high-$^{3}He/^{4}He$ mantle reservoir, peridotite, MORB-eclogite, recycled crust

1. Introduction

Rare lavas erupted at some intra-plate ocean islands sample a mantle component with high $^{3}He/^{4}He$, but the origin of this mantle component is not well understood (Kurz et al., 1982; Farley et al., 1992; Hanan and Graham, 1996; Class and Goldstein, 2005; Parman et al., 2005; Parman, 2007; Albarède, 2008; Jackson et al., 2010; Jackson and Carlson, 2012; Mukhopadhyay, 2012). Compared to the terrestrial upper mantle that is sampled by mid-ocean ridge basalts (MORB; 8 Ra; Graham, 2002), extremely high $^{3}He/^{4}He$ ratios are found in the solar wind (310 Ra) and the atmosphere of Jupiter (120 Ra; Mahaffy et al., 1998; Geiss et al., 2004). However, 3He/4He ratios up to 50 Ra are reported in terrestrial mantle-derived lavas (Stuart et al., 2003; Starkey et al., 2009). Lavas with high $^{3}He/^{4}He$ signature are thought to represent an early, primitive component preserved since Earth's accretion, though the precise location and composition of this reservoir is debated (Hart et al., 1992; Lee et al., 2010; Jackson et al., 2010; Coltice et al., 2011).

Owing to their association with ocean island volcanism, which is thought to result from melting of upwelling mantle plumes (Morgan, 1971), high $^{3}He/^{4}He$ lavas are thought to sample a less degassed region of the lower mantle where mantle plumes may originate (Kurz et al., 1982; Zindler and Hart, 1986; Hart et al., 1992; Class and Goldstein, 2005). If plumes originate at the core-mantle boundary (CMB), then the high $^{3}He/^{4}He$ component in plumes may reside at the bottom of the mantle. The high $^{3}He/^{4}He$ mantle reservoir was recently found to exhibit different $^{129}Xe/^{130}Xe$ than MORB and the Earth's atmosphere, which indicates that the high $^{3}He/^{4}He$ reservoir was formed during

the first 100 million years following accretion (Mukhopadhyay, 2012; Petö et al., 2013). This finding of an ancient origin for the high $^{3}He/^{4}He$ reservoir is consistent with the observation of primitive Pb-isotopic compositions in terrestrial mantle-derived lavas with the highest $^{3}He/^{4}He$ (Jackson et al., 2010). Thus, at least two lines of evidence suggest the survival of the high $^{3}He/^{4}He$ mantle domain over 4.5 Ga of Earth's evolution. Storage in the deep mantle, where viscosity is higher and convective motions are slower (Brandenburg et al., 2008; Li et al., 2014), may help to explain the long-term survival of this reservoir with primitive noble gas signatures (e.g. Jackson et al., 2010).

Regions of anomalously low seismic velocity at the base of the mantle, referred to as the large low shear velocity provinces (LLSVP), are defining features of the lower mantle (Garnero and McNamara, 2008; Torsvik et al., 2010). Recently, Labrosse et al. (2007) suggested that the LLSVPs at the core-mantle boundary (CMB) are remnants of an early basal magma ocean, and it has been suggested that this basal magma ocean may host primitive noble gas signatures (Coltice et al., 2011; Mukhopadhyay, 2012). Li et al. (2014) argue that the LLSVPs host both primitive domains with primitive noble gas signatures and domains that harbor subducted crustal materials, and the primitive and recycled reservoirs are intimately associated within the LLSVPs. If the Li et al. (2014) result is correct, then it may be difficult to sample the high $^{3}He/^{4}He$ mantle reservoir in pure form in hotspot lavas, as subducted crust may be admixed with the high $^{3}He/^{4}He$ component. Plume-fed ocean island lavas may provide a window into the composition and evolution of the deepest regions of the planet, and they may show that individual mantle plumes host both primitive and recycled components (Zindler and Hart, 1986; Hofmann, 1997), which is consistent with the suggestion that primitive and recycled components are intimately associated in the deepest mantle (Li et al., 2014). It has long been known that recycled components exhibit highly heterogenous radiogenic isotopic compositions, which reflects a diversity of subducted protoliths of different ages in hotspot lavas (Zindler and Hart, 1986; Hofmann, 1997; Stracke et al., 2005). However, lavas hosting primitive (high) $^{3}He/^{4}He$ signatures were suggested to sample a common mantle component with limited isotopic variability (Hart et al., 1992), but it is becoming apparent that high $^{3}He/^{4}He$ lavas globally exhibit rather dramatic isotopic and trace element variability (Class and Goldstein, 2005; Jackson et al., 2007; Starkey et al., 2009),

which suggests that the mantle reservoir sampled by high $^3He/^4He$ lavas is heterogeneous. Mixing recycled crust into the high $^3He/^4He$ mantle may help to explain the isotopic and trace element heterogeneity in this reservoir (Jackson et al., 2008; Gonnermann and Mukhopadhyay, 2009; Parai et al., 2009). If so, major element compositions of high $^3He/^4He$ lavas should also reflect the incorporation of recycled mafic material into their mantle source.

While the global isotopic and trace element systematics of high $^3He/^4He$ lavas have been explored (e.g. Jackson et al., 2007; Jackson et al., 2008), a systematic comparison of the major element geochemistry of lavas with the most primitive noble gas signatures has not been undertaken. Such an analysis is required to place constraints on the possible melting conditions and source compositions of high $^3He/^4He$ lavas. Major elements can help constrain the source lithology melting beneath high $^3He/^4He$ volcanoes, and can illuminate common processes that might operate during melting of the high $^3He/^4He$ component (e.g., higher temperature of melting of high $^3He/^4He$ mantle components; Putirka, 2008). In spite of the overall rarity of lavas with this primitive isotopic signature, geochemical datasets are now available on lavas at locations with high $^3He/^4He$ and it is now possible to make a systematic comparison of the major element compositions of high $^3He/^4He$ basaltic lavas from several different localities. The aim is to determine whether the high $^3He/^4He$ mantle exhibits systematic major element characteristics that may require involvement of recycled crustal components.

Here we provide an analysis of the major element compositions of global ocean island basalts (OIBs) from locations with the highest $^3He/^4He$ ratios. Lavas with $^3He/^4He$ greater than 30 Ra (ratio to atmosphere, where the atmospheric $^3He/^4He$ is 1.384×10^{-6}), are found at four locations: Hawaii (e.g. Kurz et al., 1982, 1983; Valbracht et al., 1997; Moreira et al., 2001; Mukhopadhyay et al., 2003; Keller et al., 2004; Clague and Calvert, 2009; Garcia et al., 2012), Galapagos (Graham et al., 1993; Kurz and Geist, 1999; Jackson et al., 2008; Kurz et al., 2009), Samoa (Farley et al., 1992; Workman et al., 2004; Jackson et al., 2007, 2009; Hart and Jackson, 2014) and Iceland (e.g. Condomines et al., 1983; Kurz et al., 1985; Hilton et al., 1999; Dixon et al., 2000; Moreira et al., 2001; Macpherson et al., 2005; Füri et al., 2010). Lavas with the highest $^3He/^4He$ ratios globally

are found in the 62 million-year-old (Saunders et al., 1997) flood basalt province located on Baffin Island and West Greenland (BIWG) (e.g. Graham et al., 1998; Stuart et al., 2003; Starkey et al., 2009), and this flood basalt is thought to be related to the proto-Iceland plume. All four locations with high $^{3}He/^{4}He$, Hawaii, Samoa, Galapagos, and Iceland are located over the periphery of the LLSVPs (large low shear-wave velocity provinces) (Figure 1). Hawaii, Samoa and Galapagos bracket the northern, western and eastern margins of the Pacific LLSVP, and Iceland brackets the northern margin of the Atlantic LLSVP, thus possibly providing a geographically diverse sampling of this lower mantle feature, if the source of the basalts on these islands is indeed rooted to the base of the mantle (Torsvik et al., 2010) (however, the relationship between LLSVPs and hot-spots is not universally accepted, Austermann et al., 2014). Additionally, these four hotspots are erupted in diverse tectonic environments on both young and old oceanic lithosphere. Consistent with the isotopic and geographic diversity in high $^{3}He/^{4}He$ lavas, we show that their major element compositions are highly heterogeneous and argue that these lavas result from melting heterogeneous mantle sources under diverse melting conditions. We find that lavas from locations with the highest $^{3}He/^{4}He$ at three of the ocean islands−Galapagos, Hawaii and Samoa−have elevated titanium concentrations that cannot be generated by melting a primitive, undifferentiated peridotite reservoir (e.g. Dasgupta et al., 2006; Prytulak and Elliot, 2007; Gerbode and Dasgupta, 2010; Dasgupta et al., 2010), but instead require a Ti-rich component, likely recycled oceanic crust. The elevated Ti concentrations in high $^{3}He/^{4}He$ lavas relate to higher $^{206}Pb/^{204}Pb$ ratios in the same lavas, which is also consistent with recycling of oceanic crust.

2. Treatment of geochemical data

The geochemical database of major elements and isotopes from global OIBs from Jackson and Dasgupta (2008) is used to provide a global reference for the major element variability in OIBs (Supplementary Table 1). This high quality, filtered dataset provides coupled measurements of radiogenic isotopes and major elements on the freshest, least evolved OIB samples, which facilitates estimating primary magma compositions and relating these melt compositions to mantle source variability inferred from their isotopic variability.

148 The major element compositions associated with the highest $^{3}He/^{4}He$ lavas
149 globally were obtained for lavas from four active hotspots (Hawaii, Iceland, Galapagos
150 and Samoa) and a flood basalt associated with the proto-Iceland plume (Baffin Island and
151 West Greenland (BIWG)). At Hawaii, Galapagos and Samoa, the volcanoes with the
152 highest $^{3}He/^{4}He$ are selected for comparison with the global OIB database, as it is critical
153 to target and evaluate the major element composition of lavas originating from the high
154 $^{3}He/^{4}He$ mantle reservoir. At Hawaii, Galapagos and Samoa, the volcanoes with the
155 highest $^{3}He/^{4}He$ (Loihi, Fernandina and Ofu, respectively) are relatively young (< 1
156 million years old; McDougall, 2010; Garcia et al., 2006; Geist et al., 2006; Kurz et al.,
157 2009; Koppers et al., 2011) and are located at or near the active end of the
158 respective "hotspot" track. Paired $^{3}He/^{4}He$ and major element and heavy radiogenic
159 isotopic (i.e., $^{87}Sr/^{86}Sr$, $^{143}Nd/^{144}Nd$, $^{206}Pb/^{204}Pb$) data are not available on most lavas
160 from these three volcanoes, but lavas from each volcano are found to exhibit elevated
161 $^{3}He/^{4}He$. Therefore, to augment the geochemical dataset for this analysis, both lavas with
162 helium isotopic measurements and lavas that lack $^{3}He/^{4}He$ data from Loihi, Fernandina
163 and Ofu are used for evaluating the major element composition of the high $^{3}He/^{4}He$
164 reservoir from each respective ocean island. The geochemical data for Loihi, Fernandina
165 and Ofu that were used in this study are from Georoc database (http://georoc.mpch-
166 mainz.gwdg.de/georoc) and shown in Supplementary Table 1. We emphasize that the
167 $^{3}He/^{4}He$ of most lavas examined here are not known, as $^{3}He/^{4}He$ measurements are
168 relatively rare while major element data required for our analysis are common in the
169 literature.

170 Unlike Hawaii, Galapagos and Samoa, which have individual volcanic centers
171 that are associated with elevated $^{3}He/^{4}He$, lavas with the highest $^{3}He/^{4}He$ (>30 Ra) in
172 Iceland are located in the late Tertiary basalts in the northwest portion of the island
173 (Hilton et al., 1999), and are not associated with specific volcanic centers. The Icelandic
174 tertiary basalts remain poorly characterized for helium isotopic compositions (Breddam
175 and Kurz, 2001; Graham, 2002; Harlou, 2007); only a single lava with $^{3}He/^{4}He > 30$ Ra
176 has been identified in outside of the Tertiary basalts of northwest Iceland (Macpherson et
177 al., 2005). Therefore, instead of taking the approach of using specific volcanic centers as
178 representative of the high $^{3}He/^{4}He$ component in Iceland−which is the approach taken for

characterizing melts of the high $^3He/^4He$ mantle at Hawaii, Galapagos and Samoa−we limit our analysis in Iceland to samples from the Tertiary province with $^3He/^4He > 30$ Ra; the database for Iceland Tertiary lavas with paired major element analyses and $^3He/^4He >$ 30 Ra is limited to only 3 samples (Hilton et al., 1999; Harlou, 2007; Jackson et al., 2008), and they provide a preliminary characterization of the high $^3He/^4He$ component beneath Iceland. The highest $^3He/^4He$ lavas globally (up to 50 Ra) are reported from the flood basalt province in Baffin Island and West Greenland (BIWG), which was erupted at 62 Ma and is associated with the proto-Iceland plume (e.g. Francis, 1985; Robillard et al., 1992; Graham et al., 1998; Stuart et al., 2003; Kent et al., 2004; Starkey et al., 2009; Larsen and Pedersen, 2009). Owing to their age, the $^3He/^4He$ ratios in the BIWG samples have experienced variable ingrowth of ^4He since eruption, and some of the BIWG lavas have relatively low $^3He/^4He$. Jackson et al. (2010) found a relationship between $^3He/^4He$ and helium concentrations that supports this hypothesis, and they showed that post-eruptive ingrowth of radiogenic helium is likely responsible for the relatively low $^3He/^4He$ observed in some of the BIWG samples, as these samples are helium-poor. Owing to eruption through continental crust, many BIWG lavas have experienced crustal assimilation, which perturbs their isotopic compositions away from mantle compositions (e.g. Larsen and Pedersen, 2009). However, Larsen and Pedersen (2009) used major and trace element proxies for assimilation to identify lavas that have experienced the least assimilation, and they found that such lavas tend to plot in a tight cluster in Pb isotopic space. A subset of geochemically well-characterized lavas from the BIWG have also been characterized for their Pb-isotopic compositions, which is necessary for evaluating a role for crustal assimilation, and this subset of lavas is argued to have experienced minimal assimilation (Graham et al., 1998; Jackson et al., 2010) and is shown in all relevant figures. Additionally, a larger geochemical dataset for BIWG lavas characterized for $^3He/^4He$ is available on lavas that have not been characterized for the Pb-isotopic compositions (Stuart et al., 2003; Starkey et al., 2009), and these data are shown separately in the relevant figures.

To estimate primary melt compositions, low MgO lavas (< 8 wt.% for Loihi, Fernandina and BIWG, and < 10 wt.% for Ofu) were excluded, as such lavas can be affected by clinopyroxene and plagioclase fractionation. The major element compositions

of the remaining lavas are affected primarily by fractionation or accumulation of olivine (as evidenced by horizontal data trends in MgO vs. CaO/Al_2O_3 plot) (Figure 2). The lavas were renormalized to 100 wt.% with all iron reported as FeO_{total}. Lavas were corrected for olivine fractionation/addition in 0.05 wt.% increments until they were in equilibrium with mantle olivine of forsterite content 90 (i.e., Fo_{90}). Equilibrium olivines were generated allowing olivine-melt K_d to vary with the composition based on the parameterization of Tamura et al. (2000) presented in Lee et al. (2009) and assuming molar $Fe^{3+}/Fe_T = 0.1$.

For comparison we also included 43 MORB glass samples with the highest MgO concentrations, between 8.8 to 10.45 wt.% MgO, which include 17 glass samples from Siqueiros (Perfit et al., 1996) and 26 glass samples with the highest MgO from Melson et al. (2002). These MORB samples are sufficiently primitive that they are affected only by olivine fractionation. The MORB samples are also olivine fractionation corrected to be in equilibrium with Fo_{90} olivine and the corrected major element compositions of the Siqueiros lavas are similar to the 26 glass samples with the highest MgO from Melson et al. (2002).

3. Data and observations

Hawaii and Samoa are both located on a corridor of mature Pacific plate lithosphere of approximately the same age (100 Ma), the Galapagos Islands are situated on a relatively young portion of the Nazca plate < 200 km from the Galapagos Spreading Center, and Iceland is a ridge-centered hotspot. The BIWG lavas were erupted at the site of rifting in the Labrador Sea and Baffin Bay, where the lithosphere had been thinned by rift-related extension (e.g. Clarke and Upton, 1971). While Hawaii is located far from any plate boundary, Iceland and the Galapagos are erupted at or near mid-ocean ridges, and Samoa is located < 100 km from the northern terminus of the Tonga trench. Therefore, while sampling geographically diverse locations in the Atlantic and Pacific (Figure 1), the three hotspots are located in tectonically different environments and are situated on top of oceanic lithosphere that is of different thickness (Dasgupta et al., 2010). In the context of the global OIB dataset (Jackson and Dasgupta, 2008), below we present the

major element and isotopic compositions of high $^3He/^4He$ OIB lavas from Hawaii, Galapagos, Samoa, Iceland and the BIWG flood basalts.

Figure 2 shows variation diagrams of MgO vs. major element oxides for global OIBs and MORBs with high $^3He/^4He$ lavas highlighted separately. BIWG flood basalt lavas are also shown. From the diagrams, it is apparent that the high $^3He/^4He$ lavas from different localities encompass much of the major element variability observed in global OIBs; fractionation of clinopyroxene from the high $^3He/^4He$ lavas is not evident down to 8% MgO (10% MgO for Ofu), suggesting that the major element variability is driven primarily by olivine fractionation or accumulation. Compared to other high $^3He/^4He$ localities, Ofu defines a compositional extreme with low SiO_2, low Al_2O_3 and low CaO and the highest TiO_2 and FeO_T at a given MgO (at a given MgO, the FeOT tends to show significant variability, and this is also observed in Fernandina lavas). At the other extreme, lavas from the BIWG - Iceland suite have high SiO_2 (and possibly higher CaO) and low TiO_2 and FeO_T at a given MgO; Iceland has Al_2O_3 that is offset from BIWG lavas and overlaps with Ofu, though we note that the number of high $^3He/^4He$ samples from Iceland are few. The BIWG-Iceland suite exhibits major element trends in Figure 2 that extend to the MORB field, but FeO_T is a notable exception, which tends to be higher in BIWG-Iceland lavas than MORB at a given MgO. Loihi and Fernandina have SiO_2 and TiO_2 concentrations at a given MgO that are compositionally intermediate in comparison to the extreme compositions from the Ofu (low SiO_2) and the BIWG-Iceland suite (high SiO_2). However, Loihi and Fernandina have different Al_2O_3 and FeO_T concentrations at a given MgO: Al_2O_3 and FeO_T in Fernandina lavas are lower (more MORB-like) than in Loihi, where the Al_2O_2 and FeO_T concentrations approach those found in Ofu lavas. The total alkali vs. silica (TAS) figure shows that high $^3He/^4He$ lavas from only two locations, Ofu and a subset of Loihi samples, exhibit alkalic compositions, and these are the two high $^3He/^4He$ locations situated furthest from ridges. Only Loihi exhibits both tholeiitic and alkalic lavas. Lavas from the other high $^3He/^4He$ locations (Fernandina and the BIWG-Iceland suite) are tholeiitic, and are located near ridges.

Major element compositions for lavas from high $^3He/^4He$ locations and lavas from a global OIB dataset are corrected for olivine fractionation and are presented in Figure 3.

The FeO_T vs. SiO_2 plot shows that the two major element oxides are overall negatively correlated in the global OIB dataset (Dasgupta et al., 2010). Localities known to have carbonatite flows and dikes−Cape Verde and the Canary Islands−anchor the low SiO_2 and high FeO_T portion of the global trend. The high-SiO_2 portion of the global trend has two distinct groups: geochemically-enriched tholeiitic lavas from Hawaii (this enriched Hawaiian series is anchored by lavas from Koolau, particularly the Makapuu section; Frey et al., 1994; Hauri, 1996; Huang et al., 2005; Huang and Frey, 2005; Huang et al., 2007, 2011; Jackson et al., 2012) that have higher FeO_T at a given SiO_2 and MORB that have lower FeO_T at a given SiO_2 content. The enriched-mantle end-members, EM-1 and EM-2, tend to plot in the middle of the global OIB array in a plot of SiO_2 vs. FeO_T (Jackson and Dasgupta, 2008). High $^3He/^4He$ localities span much of the global OIB array, but they do not have SiO_2 as low as those found in the OIB localities with carbonatite dikes and flows, nor they have the coupled high FeOT and high SiO_2 found in geochemically-enriched Hawaiian lavas (we note that Hawaiian lavas from Loihi are geochemically depleted and anchor the low SiO_2 portion of the Hawaiian array). Among high $^3He/^4He$ localities globally, Ofu lavas have the lowest SiO_2 (and highest FeO_T) and Loihi has somewhat higher SiO_2 (and lower FeO_T). High $^3He/^4He$ lavas from the near-ridge hotspots, Fernandina and the BIWG-Iceland suite, have the highest SiO_2 and the lowest FeO_T among high $^3He/^4He$ localities.

The global OIB trend identified in plots of SiO_2 vs. FeO_T −including the separate groups for MORB, geochemically-enriched Hawaiian lavas, and hotspot localities with carbonatite flows and dikes−is also observed in plots of SiO_2 vs. TiO_2, FeO vs.TiO_2, SiO_2 vs.Na_2O/TiO_2 and SiO_2 vs. CaO/Al_2O_3 (Figure 3). In addition to having high FeO_T and low SiO_2, ocean island localities with carbonatite flows and dikes have high CaO/Al_2O_3, high TiO_2, and low Na_2O/TiO_2. While high $^3He/^4He$ lavas at several ocean islands do exhibit elevated TiO_2, they do not have SiO_2 as low as and CaO/Al_2O_3 as high as those observed at ocean island localities with outcropping carbonatite. The high SiO_2-portion of the various major element trends, defined by geochemically-enriched Hawaiian lavas and MORB, have the lowest TiO_2 and CaO/Al_2O_3; however, geochemically enriched Hawaiian lavas have lower Na_2O/TiO_2 and higher FeO_T and TiO_2 at a given SiO_2 than MORB. High $^3He/^4He$ lavas span much of the global range in TiO_2, where Ofu has the

highest TiO_2 among high $^3He/^4He$ localities and the BIWG-Iceland suite has the lowest TiO_2, while Loihi and Fernandina lavas have similar, intermediate TiO_2 concentrations. Fernandina and the BIWG-Iceland suite, which erupted in extensional settings (at a ridge or near a ridge), tend to form major element trends that are anchored by MORB. However, TiO_2 in Fernandina is a clear exception, as Fernandina is erupted near a ridge yet has TiO_2 that is similar to Loihi, which is erupted on 100-Ma oceanic lithosphere.

Sr, Nd and Pb isotopic data of global OIB and high $^3He/^4He$ lavas are shown in Figure 4. In $^{207}Pb/^{204}Pb$ vs. $^{206}Pb/^{204}Pb$ plot, BIWG lavas plot near the 4.5-Ga geochron. High $^3He/^4He$ lavas from other locations are translated to the right of the geochron to radiogenic Pb-isotopic compositions. Ofu and Fernandina have the most radiogenic Pb-isotopic compositions while Loihi and the Iceland high $^3He/^4He$ lavas do not extend to the high Pb-isotopic values found at the Samoa and Hawaii high $^3He/^4He$ localities. In the $^{143}Nd/^{144}Nd$ vs. $^{206}Pb/^{204}Pb$ plot, high $^3He/^4He$ lavas are shifted to a lower (more geochemically enriched) range of $^{143}Nd/^{144}Nd$ ratios than observed in average MORB from Gale et al. (2013). Ofu, which has the highest $^{206}Pb/^{204}Pb$ compositions in the suite of high $^3He/^4He$ lavas, has among the lowest $^{143}Nd/^{144}Nd$ values observed among high $^3He/^4He$ OIB localities; in $^{87}Sr/^{86}Sr$ vs. $^{206}Pb/^{204}Pb$ plot, Ofu similarly exhibits a high $^{87}Sr/^{86}Sr$ composition. In summary, there is significant isotopic heterogeneity sampled by locations with the highest $^3He/^4He$.

Figure 5 depicts relationships between $^{206}Pb/^{204}Pb$ versus olivine fractionation corrected SiO_2, CaO/Al_2O_3, and TiO_2, for global OIBs and high $^3He/^4He$ intraplate volcanism localities. As noted above, high $^3He/^4He$ localities span a large portion of the global OIB variability. However, high $^3He/^4He$ lavas do not exhibit the extremely high $^{206}Pb/^{204}Pb$ found at localities with radiogenic Pb-isotopic (i.e., HIMU, high μ, where $\mu = {}^{238}U/^{204}Pb$) compositions and the high CaO/Al_2O_3 and low SiO_2 found at localities with carbonatite dikes and flows. Notably, the TiO_2 abundances in the lavas from the high $^3He/^4He$ localities tend to increase with increasing $^{206}Pb/^{204}Pb$.

4. Discussion

We find that the various localities where $^{3}He/^{4}He > 30$ Ra has been reported−Loihi (Hawaii), Fernandina (Galapagos), Ofu (Samoa) and the high $^{3}He/^{4}He$ lavas of the BIWG-Iceland suite−exhibit a wide range of major element and isotopic compositions. The isotopic variability in high $^{3}He/^{4}He$ lavas indicates that the mantle sources of high $^{3}He/^{4}He$ lavas are heterogeneous and have different time-integrated histories (Jackson et al., 2007), while the major element variability at high $^{3}He/^{4}He$ localities stems from both heterogeneous mantle sources (possibly representing mixtures of multiple mantle sources with heterogeneous compositions) and variable melt processes.

4.1. Isotopic heterogeneity in the highest $^{3}He/^{4}He$ lavas globally

High $^{3}He/^{4}He$ ratios represent a geochemical signature that is thought to be a primordial isotopic fingerprint in the solar system. However, the high $^{3}He/^{4}He$ mantle reservoir sampled at intraplate magmatic centers is found to exhibit $^{143}Nd/^{144}Nd$ compositions that are offset to values higher (more geochemically depleted) ratios than chondrites, the presumed building blocks of the terrestrial planets. Thus, the mantle reservoir with the highest, (i.e., most primitive) $^{3}He/^{4}He$ does not have chondritic $^{143}Nd/^{144}Nd$, but instead preserves a history of long-term geochemical depletion. The presence of primitive noble gas signatures in a mantle domain characterized by long-term geochemical depletion is paradoxical, and has been the subject of significant discussion (Hart et al., 1992; Farley et al., 1992; Hanan and Graham, 1996; Parman et al., 2005; Class and Goldstein, 2005; Parman, 2007; Albarède, 2008; Gonnermann and Mukhopadhyay, 2009; Lee et al., 2010) since the discovery of high $^{3}He/^{4}He$ in OIB (Kurz et al., 1982; Rison and Craig, 1983).

A discovery made nearly a decade ago may shed new light on the origin of the high $^{3}He/^{4}He$ mantle. Boyet and Carlson (2005) observed that modern terrestrial mantle-derived lavas have $^{142}Nd/^{144}Nd$ that is 18 ± 5 ppm higher than ordinary (O) chondrites (Carlson and Boyet, 2008), and they argued that this was the result of an early differentiation event in the Earth that occurred within 30 million years after accretion (or possibly within 20 million years of accretion, using a recently-determined ^{146}Sm half-life; Kinoshita et al., 2012). This early differentiation event generated two complementary

357 reservoirs called the early depleted (EDR) and early enriched (EER) reservoirs (Boyet
358 and Carlson, 2005, 2006). The former reservoir inherited superchondric Sm/Nd and
359 generated superchondritic $^{142}Nd/^{144}Nd$ and $^{143}Nd/^{144}Nd$, while the latter reservoir
360 inherited subchondritic Sm/Nd and generated subchondritic $^{142}Nd/^{144}Nd$ and $^{143}Nd/^{144}Nd$.
361 To generate a $^{142}Nd/^{144}Nd$ ratio that is 18 ppm higher than O-chondrites, the Sm/Nd of
362 the EDR is calculated to be 5-7 % higher than chondrites, which results in a present-day
363 $^{143}Nd/^{144}Nd$ of 0.5130 ± 0.0001. The EDR is argued to preserve high $^{3}He/^{4}He$, and
364 surviving remnants of the EDR are suggested to melt beneath hotspots and give rise to
365 high $^{3}He/^{4}He$ lavas (Caro et al., 2008; Carlson and Boyet, 2008; Caro and Bourdon, 2010;
366 Jackson et al., 2010; Jackson and Carlson, 2011, 2012). This hypothesis is supported by
367 the observation that lavas from the same location as the highest $^{3}He/^{4}He$ lavas globally
368 (50 Ra, erupted at BIWG at 62 Ma as part of the proto-Iceland plume; Graham et al.,
369 1998; Stuart et al., 2003; Starkey et al., 2009) have $^{143}Nd/^{144}Nd$ that is within the range
370 predicted for the EDR and Pb-isotopic compositions that plot near the Geochron, the
371 locus of data in Pb-isotopic space defined by reservoirs that have had unfractionated
372 U/Pb ratios for 4.5 Ga. However, incomplete mixing of nucleosynthetic anomalies in
373 the solar nebula may have generated $^{142}Nd/^{144}Nd$ variability in the chondrite reservoir that
374 is not due to the decay of ^{146}Sm (Ranen and Jacobsen, 2006) and this is a subject of
375 ongoing work (Andreasen and Sharma, 2007; Carlson et al., 2007; Qin et al., 2011;
376 Huang et al., 2013; Sprung et al., 2013).

377 A recent discovery finds that high $^{3}He/^{4}He$ lavas from the modern Iceland plume
378 have $^{129}Xe/^{130}Xe$ ratios that are distinct from the depleted MORB mantle and the
379 atmospheric value (Mukhopadhyay, 2012; Petö et al., 2013), which supports the
380 hypothesis that the high $^{3}He/^{4}He$ mantle reservoir formed within 100 million years
381 following accretion. This time period brackets, and is therefore consistent with, the
382 timing of the EDR's formation within 20-30 million years after accretion.

383 However, lavas with the highest $^{3}He/^{4}He$ (i.e. > 30 Ra) erupted at all other
384 localities, including Hawaii, Galapagos, Samoa and Iceland, exhibit significant isotopic
385 diversity that deviates from that found in the BIWG flood basalts. First, high $^{3}He/^{4}He$
386 lavas from these localities have Pb-isotopic compositions that are displaced to the right of

the Geochron. Jackson et al. (2010) argued that the Pb-isotopic composition of the high $^{3}He/^{4}He$ lavas from Hawaii, Iceland, Galapagos and Samoa are shifted to the right of the geochron as a result of the incorporation of recycled material into the high $^{3}He/^{4}He$ mantle domain. Recycled oceanic crust has long been argued to exhibit radiogenic Pb-isotopic compositions that plot to the right of the geochron (e.g., Chase, 1981; Hofmann and White, 1982; Zindler et al., 1982), and due to the high Pb-concentration of recycled materials relative to mantle peridotite, Jackson et al. (2010) argued that admixture of recycled crust into the high $^{3}He/^{4}He$ reservoir can perturb the peridotite-crust hybridized mantle sources to the right of the geochron.

Jackson et al. (2010) also argued that recycled crustal materials are also rich in U and Th, and ^{4}He ingrowth over time will tend to diminish the $^{3}He/^{4}He$ of the mixture, a mechanism that may explain the lower $^{3}He/^{4}He$ in Hawaii, Iceland, Galapagos and Samoa lavas with primitive helium relative to extremely high $^{3}He/^{4}He$ found in BIWG lavas. The higher $^{87}Sr/^{86}Sr$ (and lower $^{143}Nd/^{144}Nd$) in Samoan lavas relative to all other hotspot localities with high $^{3}He/^{4}He$ may relate to the incorporation of recycled sediment into the Samoan high $^{3}He/^{4}He$ mantle source, but the origin of this sediment is ancient (Jackson et al., 2007) and does not relate to the incorporation of modern marine sediment from the Tonga subduction zone into the Samoan mantle, as suggested previously (Farley, 1995). Thus, the addition of recycled oceanic crust, with or without sediment, to the high $^{3}He/^{4}He$ EDR has been invoked to explain the isotopic shift away from EDR compositions that is observed in OIBs (but not BIWG lavas) with the highest $^{3}He/^{4}He$ globally (Jackson et al., 2010).

The key observation is that high $^{3}He/^{4}He$ localities exhibit isotopic differences from each other (Figure 4), which indicates heterogeneous mantle sources contributing melt to high $^{3}He/^{4}He$ lavas globally. Jackson et al. (2007) argued that the high $^{3}He/^{4}He$ mantle source is sampled in relatively pure form (i.e., without the admixture of recycled crustal materials) in BIWG lavas, but this is a rare occurrence. Recent dynamic models may provide an explanation for why the high $^{3}He/^{4}He$ reservoir is rarely sampled in pure form. The numerical simulations of Li et al. (2014) suggest that there is an intimate association of recycled crustal materials and material with high $^{3}He/^{4}He$ in the deep

mantle; if this reflects the geometry of the high and low $^{3}He/^{4}He$ reservoirs in the sources of mantle plumes, then the high $^{3}He/^{4}He$ mantle reservoir may be sampled only rarely in pure form, such as the example provided in the BIWG suite. Thus, high $^{3}He/^{4}He$ lavas erupted at Hawaii, Galapagos, Samoa and Iceland, which exhibit Pb-isotopic compositions that are shifted to the right of the (4.5 Ga) Geochron, may be melts hybrid lithologies comprising both the high $^{3}He/^{4}He$ reservoir and low $^{3}He/^{4}He$ recycled components. If the isotopic variability in different high $^{3}He/^{4}He$ OIBs results from the incorporation of recycled materials (recycled oceanic crust with or without sediments) into the high $^{3}He/^{4}He$ peridotitic reservoir, the signature of recycled materials should also be evident in the major element compositions of high $^{3}He/^{4}He$ lavas. Below, we examine the major element compositions of high $^{3}He/^{4}He$ lavas globally and show that some of their major element variability can be explained by conditions of melting and melt-rock interaction in a mixed peridotite-eclogite system that are modulated, in part, by the thickness of the lithosphere during the time of eruption. We also build on the work of Prytulak and Elliot (2007) and, following the arguments of several others (e.g. Dasgupta et al., 2006, 2010; Gerbode and Dasgupta, 2010; Mallik and Dasgupta, 2012), show that the mantle sources of several high $^{3}He/^{4}He$ locations have TiO_2 concentrations that are too high to be explained by melting either a depleted peridotite or a primitive mantle peridotite under volatile-free conditions. The TiO_2-enrichment in the mantle sources of these lavas is best explained by the incorporation of a mafic component into the high $^{3}He/^{4}He$ mantle reservoir, a process that can also explain the elevated $^{206}Pb/^{204}Pb$ in high $^{3}He/^{4}He$ lavas from Loihi, Fernandina, Ofu and Iceland.

5. Major element heterogeneity in high $^{3}He/^{4}He$ lavas globally

5.1. Major element concentrations in OIB: Influence of LAB thickness and source composition

Lavas erupted at high $^{3}He/^{4}He$ localities globally exhibit a wide range in radiogenic isotopic compositions that spans much of the global OIB dataset, and the major element compositions of high $^{3}He/^{4}He$ lavas also show diverse compositions. Dasgupta et al. (2010) examined major element variability in the global OIB dataset and compared the variability to experimental results of melting a volatile-free peridotite. The

447 authors identified clear patterns in the major element data that can be used to evaluate the
448 diversity of major element compositions found in high $^3He/^4He$ lavas.

449 In a plot of FeO_T vs. SiO_2, for example, Dasgupta et al. (2010) argued that the
450 negative correlation in the global OIB dataset can be explained, only in part, by different
451 average pressures of melting of a volatile-free peridotite source; primary melts generated
452 from higher average pressures of melting have higher FeO_T and lower SiO_2 compared to
453 primary melts generated at lower average pressures of melting (e.g. Langmuir et al.,
454 1992). However, Dasgupta et al. (2010) noted that the slope of the negatively correlated
455 FeO_T -SiO_2 trend, observed in fractionation-corrected OIBs, is too shallow to be caused
456 by different pressures of melting of a homogeneous, volatile-free peridotite source
457 (Figure 3). In particular, the extremum of the trend--one is defined by high FeO_T and low
458 SiO_2 (found at the Canary and Cape Verde Islands) and the another is defined by SiO_2
459 that is as high as MORB and higher than MORB FeO_T (found in Koolau Makapu'u lavas
460 from Hawaii)--cannot be generated by partial melting of volatile-free peridotite alone.
461 The former is suggested to result from melting a carbonated mantle with contributions
462 from mafic lithologies (as observed in OIB localities with carbonatite outcrops at the
463 Canary and Cape Verde Islands; Dasgupta et al., 2006; Gerbode and Dasgupta, 2010;
464 Mallik and Dasgupta, 2013, 2014), and the latter is thought to result from melting, melt-
465 rock reaction, and remelting involving a SiO_2-saturated lithology such as MORB-eclogite
466 and peridotite (e.g., Hauri, 1996; Sobolev et al., 2005), and is observed only in
467 geochemically-enriched Hawaiian lavas. Lavas erupted at high $^3He/^4He$ localities also
468 define a negative trend in the global FeO_T-SiO_2 trend. Although the high $^3He/^4He$ lavas
469 do not extend to the extremely low SiO_2 compositions such as melilitite or melilititic
470 nephelinite as found in Canary and Cape Verde, or the elevated FeO_T at high SiO_2 found
471 in geochemically-enriched Hawaiian lavas (thought to be caused by MORB-eclogite
472 melting at depths), compositions of some of the $^3He/^4He$ basalts cannot be generated by
473 melting of volatile-free peridotite either.

474 In Figure 3, we identify additional major element trends in the global OIB dataset
475 that, like the FeO_T vs. SiO_2 trend, reflect, in part, average pressures of melting and
476 corresponding variations in degree of melting: SiO_2 exhibits negative correlations with

TiO_2 and CaO/Al_2O_3 and a positive relationship with Na_2O/TiO_2, while FeO_T exhibits a positive relationship with TiO_2. Signatures for hybrid pyroxenite melting and involvement of MORB-eclogite (enriched Hawaiian lavas) and signatures for carbonated mantle melting (Canary and Cape Verde Islands) contribute additional variability to the overall trends. Notably, the two ocean island localities where erupted carbonatites are observed have among the highest TiO_2 in the global dataset. While high $^3He/^4He$ basalts do not extend to TiO_2 as high as some basalts in Cape Verde and Canaries, several $^3He/^4He$ localities, in particular Ofu, also tend to exhibit elevated TiO_2; Ofu in particular has relatively low SiO_2 and relatively high CaO/Al_2O_3, but Ofu does not exhibit the extreme SiO_2 and CaO/Al_2O_3 compositions found at the Canary and Cape Verde islands. Geochemically-enriched lavas from Hawaii that exhibit elevated FeO_T at the SiO_2-rich portion of the global array (found in most geochemically-extreme form in Koolau Makapuu lavas) exhibit low Na_2O/TiO_2 and high TiO_2 at high SiO_2 concentrations. High $^3He/^4He$ lavas do not exhibit these latter characteristics: High $^3He/^4He$ lavas with the highest SiO_2 globally (with SiO_2 as high as Koolau Makapu'u lavas), encountered at ridge or near-ridge settings (Galapagos and the BIWG-Iceland suite), generally have high Na_2O/TiO_2 and low TiO_2 and FeO_T and trend toward the field defined by primitive MORB.

Dasgupta et al. (2010) argued that, while source effects, including the presence of carbonated lithologies or eclogite, modulate major element variability in OIB, the average pressure of melting is also an important control on the global major element compositions in hotspot lavas. The average pressure of melting is related to the depth of lithosphere-asthenosphere boundary (LAB) at the time of volcanism, since the lithosphere represents a barrier to mantle upwelling and to the associated decompression melting of the mantle, and melting stops once LAB is approached. Because the depth of LAB is related to the age of the oceanic lithosphere, the average depth of melting, and thus the compositions of erupted hotspot lavas, relate to the age of the lithosphere at the time of oceanic volcanism (Ellam, 1992; Haase, 1996; Prytulak and Elliot, 2007; Dasgupta et al., 2010). Dasgupta et al. (2010) showed that major elements abundances (SiO_2, FeO_T , TiO_2) and ratios (Na_2O/TiO_2 and CaO/Al_2O_3) in OIB relate to the age of the oceanic lithosphere at the time of intraplate volcanism, and therefore the average

pressure of melting: MORBs and near-ridge hotspots lavas tend to have high SiO_2 and high Na_2O/TiO_2 and low FeO_T , CaO/Al_2O_3, TiO_2; hotspot lavas erupted far from ridges where the LAB is thicker have more variable major compositions than near-ridge OIBs, but exhibit some of the lowest SiO_2 and Na_2O/TiO_2 and highest FeO_T , CaO/Al_2O_3 and TiO_2. Dasgupta et al. (2010) concluded that peridotite melting alone cannot produce the major element variability observed in the global OIB dataset, particularly at OIB localities erupted on a thick oceanic plate, and they argued for a role for a greater contribution from melting of mafic lithologies where the LAB is thicker. Where the LAB is thicker, the presence of mafic lithologies with greater solidii depths than average fertile peridotite will contribute a greater proportion to the final erupted OIB melt than localities where the LAB is thinner and a greater fraction of peridotite melting can occur (Figure 6). A second observation of Dasgupta et al. (2010) is that the TiO_2 of OIB lavas erupted on old, thick oceanic plates is more variable but extends to higher concentrations than found in near-ridge hotspot lavas, and the high TiO_2 concentrations require a TiO_2-rich mafic lithology such as recycled oceanic crust in the mantle source (Prytulak and Elliot, 2007). These observations have important implications for the history and composition of the mantle source tapped by high $^3He/^4He$ hotspot localities. We emphasize that we cannot explain every aspect of the high $^3He/^4He$ data. For example, in the plots of TiO_2 vs. FeO_T and TiO_2 vs. SiO_2 (Figure 3) and TiO_2 vs. pressure (Figure 7), the high $^3He/^4He$ lavas plot within the global field, but the trends of each high $^3He/^4He$ locations are not parallel to the global trends. We cannot explain these subtrends within the global dataset, but we note that the global trend is composed of data from many hotspots localities that, like high $^3He/^4He$ lavas, do not necessarily form trends oriented with the global trend.

5.2. A mafic source component with or without carbonation in lavas with high $^3He/^4He$: Evidence from TiO_2

The estimated primary melt TiO_2 concentrations found in lavas at the two high $^3He/^4He$ localities erupted on old oceanic plate−Loihi (Hawaii) and Ofu (Samoa)−are elevated, as are TiO_2 concentrations from Fernandina lavas erupted on younger oceanic plate located < 200 km from a spreading center (Figures 2, 3, 5 and 7). TiO_2 concentrations from the other high $^3He/^4He$ localities, BIWG and Iceland, are the lowest

among high $^{3}He/^{4}He$ lavas globally; this may relate to melting under thinned lithosphere undergoing extension and rifting (BIWG) or at a spreading center (Iceland), where the degree of melting will be higher and the proportion of mafic lithologies contributing to melting will be lower (Figure 7).

Many previous studies (e.g., Frey et al., 1994; Dasgupta et al., 2006; Prytulak and Elliot, 2007; Gerbode and Dasgupta, 2010; Jackson and Dasgupta, 2008) argued that TiO_2 concentrations in many OIBs in the global dataset are too high to be generated by melting of a fertile peridotite, even at infinitesimally small degrees of melting of primitive peridotite (McDonough and Sun, 1995). We find that the observations made by these authors extend to the mantle sources of lavas erupted at two high $^{3}He/^{4}He$ localities, Loihi and Ofu (Figure 8). We outline the argument for a TiO_2-rich source lithology below and show how it specifically applies to the mantle reservoir sampled by high $^{3}He/^{4}He$ lavas.

A portion of primitive mantle that has never experienced re-enrichment by addition of recycled materials (including crust and sediment, which have higher Ti concentrations than primitive mantle peridotite) should not have Ti concentrations higher than proposed for the McDonough and Sun (1995) primitive peridotite−0.22 wt.% TiO_2−and this provides an upper limit for the Ti in unadulterated mantle. However, we also note that 90% of the global OIB dataset, including all lavas from high $^{3}He/^{4}He$ localities, have $^{143}Nd/^{144}Nd$ higher (i.e., more geochemically depleted) than the chondritic reference (Prytulak and Elliot, 2007; Jackson and Carlson, 2011), which indicates long-term source depletion in incompatible elements (Class and Goldstein, 2005), likely owing to ancient melt extraction. Therefore, if OIBs with superchondritic $^{143}Nd/^{144}Nd$, including high $^{3}He/^{4}He$ lavas (Jackson and Jellinek, 2013), are melts of a purely peridotitic source that has not had recycled crust added to it, the mantle source Ti concentrations of these OIB will be lower than the McDonough and Sun (1995) primitive mantle composition. Therefore, the 0.22 wt.% TiO_2 estimate provides a firm upper limit if the high $^{3}He/^{4}He$ mantle source is composed of pure, unadulterated peridotite.

Prytulak and Elliot (2007) found that infinitesimally small degrees of melting of a primitive mantle peridotite can generate only 2.6 wt. % TiO_2 in the garnet stability field,

or 1.6 wt. % TiO_2 in the spinel stability field. We apply the Prytulak and Elliot (2007) observations to the high $^3He/^4He$ OIB dataset. First, we note that the reference TiO_2 concentrations in lavas from Ofu (4.1 %, Figure 7c) are too high to be a product of melting of primitive mantle peridotite. Employing the calculations from Prytulak and Elliott (see Figure 2 of their paper), the TiO_2 concentrations in Loihi (2.1 wt. % TiO_2) and Fernandina (2.2 wt. % TiO_2) can be generated by melting of primitive mantle peridotite if the degree of melting is infinitely small (see Figure 7c). However, both Loihi (McKenzie and O'Nions, 1991; Watson and McKenzie, 1991; Garcia et al., 1995, 2006; Prytulak and Elliot, 2007) and Galapagos (Geist et al., 2006) lavas are suggested to result from degrees of relatively high degrees of partial melting, 5% and > 3.5%, respectively. These relatively large degree partial melts of a primitive mantle peridotite will not generate the elevated Ti concentrations at Loihi and Fernandina (see Figure 7, a and c).

It is important to consider how the partition coefficient for Ti can vary to evaluate the conclusion that Ofu, Loihi and Fernandina cannot result from melting of a primitive mantle peridotite. A recent experimental study by Davis et al. (2011) resulted in lower partition coefficients of Ti in garnet stability field of peridotite from those derived by Prytulak and Elliot (2007). Davis et al. (2011) suggest that, using the new partition coefficient of Ti in garnet stability field, it is possible to obtain TiO_2 concentrations of 2 wt.% by melting a primitive mantle peridotite by < 4% in the garnet stability field. This result would imply that the TiO_2 concentrations of Fernandina lavas can be generated by peridotite melting, if Fernandina results form 3.5% melting. However, if lavas from Loihi are generated by a degree of partial melt of 5%, then the TiO_2 concentrations in Loihi melts cannot be generated by peridotite melting, even if Ti is as incompatible in garnet as suggested by Davis et al. (2011). Again, if Loihi lavas result from melting a mantle peridotite that has not had recycled crust added to the mantle source, then the Loihi mantle source is more depleted in incompatible elements (including Ti) than primitive mantle (Class and Goldstein, 2005; Prytulak and Elliot, 2007), making it even more difficult for the new partitioning data from Davis et al. (2011) to explain the elevated Ti in Loihi lavas; this argument supports the contention that Loihi lavas sample a mantle source that has be experienced addition of a Ti-rich mafic lithology. The TiO_2 concentrations in Ofu lavas are even higher than Loihi, and following the conclusions of

599 Davis et al. (2011), such elevated TiO_2 concentrations cannot be generated at any melt
600 fraction.

601 In summary, the elevated Ti concentrations at many global OIB localities, and at
602 the high $^3He/^4He$ localities of Loihi and Ofu, cannot be explained by melt extraction from
603 primitive mantle peridotite that lacks a component of recycled crust. Prytulak and Elliot
604 (2007) examined a comprehensive list of possible candidates for the source of the
605 anomalous Ti enrichment in OIBs and concluded that the most plausible candidate is
606 recycled oceanic crust. (We emphasize that, when we indicate that melts are enriched in
607 Ti, we are not necessarily implying that the Ti is more concentrated than other
608 incompatible elements with similar partitioning (e.g., the rare Earth elements) during
609 mantle melting, as these elements are frequently not reported together with Ti. Instead,
610 we are simply making an observation of Ti concentrations). Mafic material, such as
611 recycled, MORB crust, has high Ti concentrations, and a mantle hybridization process
612 involving MORB-eclogite and peridotite can sufficiently enrich Ti in the source to
613 generate the high Ti concentrations in OIB lavas. Prytulak and Elliot (2007) determined
614 that between 1-10% of recycled pyroxenite added to a primitive mantle peridotite is
615 sufficient to generate the observed elevated Ti concentrations in OIB. We note that this
616 includes the range of Ti observed in high $^3He/^4He$ lavas (Figure 6). Prytulak and Elliott
617 (2007) argued that the geochemically-depleted Sr, Nd and Hf isotopic compositions
618 observed in OIBs, including high $^3He/^4He$ OIBs, are possible with these relatively small
619 fractions of mafic crust and because recycled oceanic crust is expected to have only
620 slightly more geochemically-enriched Sr and Nd isotopic compositions than the depleted
621 mantle (Prytulak and Elliot, 2007).

622 Global OIB with elevated TiO_2 require the addition of a Ti-rich component to
623 their mantle sources, which is best explained by the addition of recycled oceanic crust;
624 the high $^3He/^4He$ localities of Ofu and Loihi require addition of a Ti-rich lithology in
625 their mantle sources to yield the elevated TiO_2 observed at these localities. The nature of
626 the mafic component added to the high $^3He/^4He$ mantle at these localities is the subject of
627 discussion. Lavas erupted at high $^3He/^4He$ localities do not trend toward the component
628 with high FeO_T at elevated SiO_2–as found in geochemically-enriched Hawaii lavas (e.g.,

Koolau Makapu'u series)−and the silica-saturated eclogite is proposed for this Hawaiian end-member is not indicated by the major element data at high $^3He/^4He$ localities. Instead, Herzberg (2010) proposed that a silica-deficient (pyroxenitic) mafic lithology has been added to the predominantly peridotitic mantle source of Loihi lavas. However, the dominant form of recycled crustal lithology in the convecting mantle must be silica-rich, MORB-like oceanic crust rather than silica-deficient mafic component, assuming that MORB-like compositions are preserved during subduction and these compositions enter the convecting mantle. Hence, a key question is whether MORB crust-peridotite hybridization and partial melting generate major element signatures of various high $^3He/^4He$ OIBs.

A critical aspect in considering the involvement of recycled, silica-excess MORB crust in a largely peridotite mantle is how the melting of both lithologies contributes to the production of primary basalts (e.g. Ito and Mahoney, 2005). Because the solidus of MORB-eclogite is significantly deeper than the solidus of volatile-free peridotite (e.g., Yasuda et al., 1994; Petermann and Hirschmann, 2003; Spandler et al., 2008), silicate partial melt extracted from MORB crust in the mantle must interact with subsolidus peridotite. Recent experiments simulating eclogite melt-peridotite reaction have shown that such interaction not only produces silica-rich hybrid pyroxenite, argued to be in the source of Koolau Makapuu series lavas, but also a wide array of reacted, residual melts with compositional attributes similar to many OIBs (e.g., Mallik and Dasgupta, 2012, 2013). For example, peridotite melting alone cannot give rise to primary alkalic magma with < 44-45 wt. % SiO_2 and TiO_2 as high as 3.0 − 5.4 wt.% (as in Ofu; Figure 8). While a carbonated peridotite source can lower the SiO_2 of partial melts to the target values observed in Ofu (Dasgupta et al., 2007, 2013), it cannot elevate the TiO_2 abundance of partial melts to the levels observed. However, a two-step process can be envisioned for alkalic lavas from both Ofu and Loihi. First, eclogite-derived andesitic partial melt reacts with the surrounding peridotite in the presence of minor CO_2, then the reacted melt is mixed with partial melt of peridotite (Mallik and Dasgupta, 2013, 2014). To derive the source characteristics of high $^3He/^4He$ lavas, we apply the eclogite melt-peridotite hybridization model of Mallik and Dasgupta (2014), where the two end member lithologies in the mantle are MORB-like eclogite and fertile peridotite and volatile

species that can be involved is CO_2. This model allows calculation of (a) the proportion of low-degree eclogite partial melt that infiltrates fertile peridotite at depths, (b) the CO_2 content of the eclogite melt-peridotite system, and (c) the proportion of peridotite partial melt that contributes to the final composition of a target alkalic basalt. For details of the model framework and underlying experimental database the readers should refer to Mallik and Dasgupta (2014). Applying the model of Mallik and Dasgupta (2014), and taking into account compositional variability of lavas from one ocean island, we estimate that Ofu alkalic lavas can be produced by a distal source with 0.85 – 1 wt.% (average 1 wt.%) bulk CO_2, where 17-36 wt.% (average 22 wt.%) of eclogite-derived melt reacts with peridotite before the reacted melt mixes with 6-31 wt.% (average 19 wt.%) of peridotite-derived partial melt relative to the hybrid melt. In comparison to this, alkalic lavas from Loihi can be generated by a similar process as Ofu, but 1 wt. % CO_2 is required in the source domain that hosts the recycled crust and 16-26 wt. % (average 24 wt.%) eclogite-derived melt reacts with ambient mantle peridotite, followed by mixing of the reacted melt with 45-58 wt. % (average 51 wt.%) peridotite-derived partial melt (Supplementary Table 1). The range in values of source characteristics indicates that a range of source CO_2 contents and eclogite melt contributions may be feasible for each hotspot locality. While the presence of CO_2 in the source of Ofu and alkalic lavas of Loihi seems necessary, a carbonated source is not likely for the tholeiites from Loihi. However, the compositions of Loihi tholeiites can be matched by partial reactive crystallization of a CO_2-free MORB-eclogite melt in a peridotite source and subsequent mixing with peridotite partial melts (Mallik and Dasgupta, 2012), but there are no existing models to quantify the relative contribution of eclogite melt and peridotite melt for tholeiites generated by a process involving MORB-eclogite in the source as described above (i.e., the parametrized model of Mallik and Dasgupta (2014) is only based on alkalic lavas). FeO_T is not fit well by the model. However, some major element source variation may account for this difference in FeO_T. Additionally, as discussed in Mallik and Dasgupta (2014), differences in fO_2 between the melting experiments used to parametrize the model and the melting conditions beneath OIB account for some of the additional offset between the model and the high $^3He/^4He$ lavas.

690 Additionally, the shift in Pb-isotopic compositions to the right of the Geochron
691 (Figure 4) to more radiogenic compositions at Ofu and Loihi further supports the addition
692 of a recycled mafic component to their mantle sources, as subducted mafic material has
693 long-been-thought to be responsible for generating the radiogenic Pb-isotopic
694 compositions in OIB (e.g., Chase, 1981; Hofmann and White, 1982; Zindler et al., 1982).
695 In support of the conclusion that subducted crust plays a role in generating high TiO_2
696 concentrations in Ofu and Loihi, we also note that increasing $^{206}Pb/^{204}Pb$ relates to
697 increasing TiO_2 at high $^{3}He/^{4}He$ localities, where both high TiO_2 and $^{206}Pb/^{204}Pb$ are
698 consistent with recycled oceanic crust. Curiously, $^{206}Pb/^{204}Pb$ ratios in Fernandina are in
699 the same range as Ofu (Figure 5). This might indicate a contribution of a mafic
700 component in generating high $^{3}He/^{4}He$ lavas at Fernandina, but the melting parameters
701 are not sufficiently constrained beneath Fernandina to require that the Ti contents in
702 Fernandina lavas result from melting a mantle source hosting silica-rich pyroxenite;
703 additionally, the possible contribution of a sediment component to the mantle source of
704 Ofu lavas complicates a direct comparison with Fernandina lavas. The thickness of an
705 oceanic plate can modulate the contribution from mafic lithologies to the final erupted
706 melt as crustal mafic lithologies have deeper solidii than peridotite (Yasuda et al., 1994;
707 Petermann and Hirschmann, 2003; Spandler et al., 2008). This may help explain the
708 identifiable presence of silica-rich pyroxenite in the high $^{3}He/^{4}He$ mantle sources of Loihi
709 and Ofu, the only two high $^{3}He/^{4}He$ localities positioned on old oceanic lithosphere (
710 100 Ma) located far from ridges.

711 Lavas erupted at locations near ridges or rifting environments, such as lavas from
712 BIWG and Iceland, where the LAB is relatively shallow and degrees of melting are high,
713 have low TiO_2 concentrations. At shallower depths peridotite melting contributes more to
714 the final erupted lavas (Figure 6). These low Ti concentrations do not necessarily imply
715 the absence of a mafic component in the source of BIWG and Iceland lavas: the Ti
716 concentrations in the BIWG-Iceland suite are too low for a mafic component to be
717 required. Shallower depths and higher degrees of melting at the Iceland suite may
718 diminish the contribution of the mafic component and source CO_2, and therefore the TiO_2
719 concentration, to the final erupted melt (Figure 8). The fact that high $^{3}He/^{4}He$ lavas from
720 Iceland, Loihi, Fernandina, and Ofu show radiogenic $^{206}Pb/^{204}Pb$ isotopic ratios shifted to

721 the right of the Geochron that may indicate the presence of crustal component in their
722 mantle sources, but Ti is not useful for evaluating the hypothesis of a mafic component in
723 Iceland high $^{3}He/^{4}He$ lavas (as the LAB is exceptionally thin and the degree of melting is
724 likely high) or Fernandina (where the LAB is likely thin and Ti can be generated at the
725 degrees of melting suggested−3.5% if extreme partition coefficients in the garnet stability
726 field are adopted). It is only at Loihi and Ofu where existing experimental partitioning
727 data and constraints on mantle melting convincingly require a Ti-rich mafic lithology in
728 the mantle source.

729 **6. Implications**

730 **6.1. Preservation of the high $^{3}He/^{4}He$ mantle signature following admixture with a**
731 **mafic component**

732 Jackson et al. (2010) argued that recycled crustal materials may be rich in U and
733 Th, and following admixture with a high $^{3}He/^{4}He$ reservoir, ^{4}He ingrowth over time will
734 tend to diminish the $^{3}He/^{4}He$ of the mixture. Relative to the BIWG suite, which has the
735 highest $^{3}He/^{4}He$ globally and plots on the Geochron in Pb-isotopic space, the highest
736 $^{3}He/^{4}He$ lavas form Hawaii, Iceland, Galapagos and Samoa have lower $^{3}He/^{4}He$ than
737 BIWG lavas and plot to the right of the Geochron. The lower $^{3}He/^{4}He$ and the more
738 radiogenic Pb in high $^{3}He/^{4}He$ lavas from Hawaii, Iceland, Galapagos and Samoa might
739 be explained by the incorporation of a component of recycled crust into the high $^{3}He/^{4}He$
740 reservoir. In contrast, the BIWG lavas may sample the high $^{3}He/^{4}He$ mantle in relatively
741 pure form (Jackson et al., 2010). Preservation of elevated $^{3}He/^{4}He$ reservoirs in the
742 mantle, even after incorporation of recycled crust, represents an important problem that
743 must be addressed if the mantle sources of Loihi and Ofu host a component of recycled
744 oceanic crust (Stracke et al., 2005; Jackson et al., 2008; Gonnermann and Mukhopadhyay,
745 2009).

746 Jackson et al. (2008) used the presence of Ti, Ta and Nb (TITAN) anomalies in
747 the highest $^{3}He/^{4}He$ lavas from Hawaii, Iceland, Galapagos and Samoa to argue for the
748 presence recycled oceanic crust in their mantle sources. The anomalies represent
749 enrichments in these three elements relative to elements with similar mineral-melt

partition coefficients during melting in the upper mantle: Ti is enriched relative to moderately incompatible rare Sm and Tb, while Nb and Ta are enriched relative to U, Th and La. Jackson et al. (2008) argued that enrichments in the TITAN elements may reflect survival of residual rutile in the subducting slab, a phase that will preferentially retain TITAN elements in the slab during subduction, while other incompatible elements, including U and Th, are lost from the slab during dehydration or melting together with loss of He (Staudacher and Allègre, 1988). This argument is supported by high-pressure experiments: Kessel et al. (2005) find that U and Th strongly partition into the fluid at pressures > 4 GPa, while the TITAN elements tend to be conserved in, or are not lost as efficiently from, the slab (but we emphasize that this is a strong function of pressure and temperature conditions in the slab). They also showed that higher temperature slabs are more susceptible to losing U and Th to the fluid.

However, despite of the loss of U and Th during subduction it is still unlikely that degassed, oceanic crust from the top of the subducting slab is the primary lithology contributing to high $^{3}He/^{4}He$ signature. Therefore, Jackson et al. (2008) propose a model in which the association of high $^{3}He/^{4}He$ with mantle reservoirs that have signatures for a small component of mafic component result from an intimate mixture of an ancient mantle peridotite and a recycled mafic crust that have been isolated from the convecting mantle and stored in the lower mantle. They model the effect of incorporation of a mafic component into a high $^{3}He/^{4}He$ peridotite and find that, if an ancient mantle peridotite has sufficiently high $^{3}He/^{4}He$ and elevated helium concentrations, elevated $^{3}He/^{4}He$ can be preserved in the mixture for several billion years during long-term storage in the mantle. Albarède and Kaneoka (2007) and Albarède (2008) suggested a model for preservation of high $^{3}He/^{4}He$ in a mafic mantle component. They argued that helium with elevated $^{3}He/^{4}He$ could diffuse from a U- and Th-poor deep mantle peridotite reservoir into very thin layers of a refractory, U- and Th-poor mafic component. The mafic component could contribute melts to high $^{3}He/^{4}He$ OIBs, and this may account for the mafic signature observed in high $^{3}He/^{4}He$ lavas. We do not advocate this model here, as the compositions of Ofu and Loihi lavas require a contribution from peridotite melting.

In a numerical simulation, Li et al. (2014) proposed that a portion of subducted oceanic crust is incorporated into primitive reservoirs in the deep mantle. The mixture of subducted crustal material and primitive material is then directly entrained into upwelling plumes. The numerical simulations suggest that the intimate association of primitive material and recycled crust in the deep mantle is conducive to entrainment of both materials in mantle plumes. The mafic lithology may be completely admixed with the peridotite lithology, such that the final lithology is a fertile peridotite (Jackson et al., 2008; Herzberg, 2010). Alternatively, if the mafic lithology survives as a distinct lithology into the melting column, and if the length-scale of the distribution of the mafic lithology is shorter than the width of the melting column beneath a hotspot, then the mafic lithology can melt together with peridotite. If the peridotite hosts elevated $^{3}He/^{4}He$ and high helium concentrations (Jackson et al., 2008), the final erupted melt can still have elevated helium concentrations, thus providing a mechanism where the high $^{3}He/^{4}He$ can be associated with melts hosting geochemical signatures indicative of recycled oceanic crust.

7. Acknowledgements

The authors acknowledge the NSF-funded CIDER program, which provided the opportunity for a group of geochemists, petrologists and experimentalists to explore and develop the ideas presented in this paper. Constructive reviews from Sujoy Mukhopadhyay and Colin Jackson are gratefully acknowledged. We thank Julie Prytulak, Dave Graham, Keith Putirka and Tim Elliott for discussion. MGJ acknowledges support from NSF grants OCE-1153894, EAR-1348082 and EAR-1145202. RD acknowledges support from NSF grant EAR-1255391.

References

Albarède, Francis. F. (2008) Rogue Mantle Helium and Neon. Science, 319(5865), 943-945, doi: 10.1126/science.1150060.

Albarède, Francis F., and Kaneoka, Ichiro (2007) Ghost primordial He and Ne. In: Goldschmidt Conference Abstracts.

Andreasen, Rasmus, and Sharma, Mukul (2007) Mixing and Homogenization in the Early Solar System: Clues from Sr, Ba, Nd, and Sm Isotopes in Meteorites. The Astrophysical Journal, 665, 874–83.

Austermann, Jacqueline, Kaye, Bryan T., Mitrovica, Jerry X., and Huybers, Peter (2014) A statistical analysis of the correlation between large igneous provinces and lower mantle seismic structure. Geophysical Journal International, 197(1), 1–9.

Boyet, Maud, and Carlson, Richard W. (2005) ^{142}Nd evidence for early (> 4.53 Ga) global differentiation of the silicate Earth. Science, 309, 576–581.

Boyet, Maud, and Carlson, Richard W. (2006) A new geochemical model for the Earth's mantle inferred from ^{146}Sm–^{142}Nd systematics. Earth and Planetary Science Letters, 250, 254-268, doi:10.1016/j.epsl.2006.07.046.

Brandenburg, J, Hauri, Erik H., van Keken, Peter E., and Ballentine Chris J. (2008) A multiple-system study of the geochemical evolution of the mantle with force-balanced plates and thermochemical effects. Earth and Planetary Science Letters, 276, 1-13, doi:10.1016/j.epsl.2008.08.027.

Breddam, Kresten, and Kurz, Mark D. (2001) Helium isotopic signatures of Icelandic alkaline lavas. In: AGU Fall Meeting.

Carlson, Richard W., and Boyet, Maud (2008) Composition of the Earth's interior: the importance of early events. Philosophical Transactions of the Royal Society, 366, 4077–4103, doi:10.1098/rsta.2008.0166.

827 Carlson, Richard W., Boyet, Maud, and M., Horan, Mary (2007) Chondrite Barium,
828 Neodymium, and Samarium Isotopic Heterogeneity and Early Earth Differentiation.
829 Science, 316(5828), 1175–8.

830 Caro, Guillaume, and Bourdon, Bernard (2010) Non-chondritic Sm/Nd ratio in the
831 terrestrial planets: Consequences for the geochemical evolution of the mantle-crust
832 system. Geochimica et Cosmochimica Acta, 74, 3333–3349.

833 Caro, Guillaume, Bourdon, Bernard, Halliday, Alex N., and Quitté, Ghylaine (2008)
834 Super-chondritic Sm/Nd ratios in Mars, the Earth and the Moon. Nature, 452, 336-339,
835 doi:10.1038/nature06760.

836 Chase, Clement G. (1981) Oceanic island Pb: Two-stage histories and mantle evolution.
837 Earth and Planetary Science Letters, 52, 277–284.

838 Clague, David A., and Calvert, Andrew T. (2009) Postshield stage transitional volcanism
839 on Mahukona volcano, Hawaii. Bulletin of Volcanology, 71(3), 313-318,
840 doi:10.1007/s00445–008.

841 Clarke, D., and Upton, B. (1971) Tertiary basalts of Baffin Island: Field relations and
842 tectonic setting. Canadian Journal of Earth Sciences, 8, 248–258.

843 Class, C., and Goldstein, Steven L. (2005) Evolution of helium isotopes in the Earth's
844 mantle. Nature, 436, 1107-1112, doi:10.1038/nature03930.

845 Coltice, Nicolas, Moreira, Manuel, Hernlund, John, and Labrosse, Stéphane (2011)
846 Crystallization of a basal magma ocean recorded by Helium and Neon. Earth and
847 Planetary Science Letters, 308, 193-199, doi:10.1016/j.epsl.2011.05.045.

848 Condomines, M., Grönvold, K., Hooker, P., Muehlenbachs, K., O'Nions, R., Óskarsson,
849 N., and Oxburgh, E.R. (1983) Helium, Oxygen, Strontium and Neodymium isotopic
850 relationships in Icelandic volcanics. Earth and Planetary Science Letters, 66, 125–136.

851 Dasgupta, Rajdeep, Hirschmann, Marc M., and Smith, Niel D. (2007) Partial melting
852 experiments of peridotite+CO_2 at 3 GPa and genesis of alkalic ocean island basalts.
853 Journal of Petrology, 48, 2093–2124.

Dasgupta, Rajdeep, Hirschmann, Marc M., and Stalker, Kathryn (2006) Immiscible transition from carbonate-rich to silicate-rich melts in the 3 GPa melting interval of eclogite + CO_2 and genesis of silica-undersaturated ocean island lavas. Journal of Petrology, 47(4), 647-671, http://dx.doi.org/10.1093/petrology/egi088

Dasgupta, Rajdeep, Jackson, Matthew G., and Lee, Cin-Ty A. (2010) Major element chemistry of ocean island basalts - conditions of mantle melting and heterogeneity of mantle source. Earth and Planetary Science Letters, 289, 377-392, doi:10.1016/j.epsl.2009.11.027.

Dasgupta, Rajdeep, Mallik, Ananya, Tsuno, Kyusei, Withers, Anthony C., Hirth, Greg, and Hirschmann, Marc M. (2013) Carbon-dioxide-rich silicate melt in the Earth's upper mantle. Nature, 493, 211-215, doi:10.1038/nature11731.

Davis, Fred A., Hirschmann, Marc M., and Humayun, Munir (2011) The composition of the incipient partial melt of garnet peridotite at 3 GPa and the origin of OIB. Earth and Planetary Science Letters, 308, 380–90.

Dixon, Eleanor T., Honda, Masahiko, McDougall, Ian, Cambell, Ian H., and Sigurdsson, Ingvar (2000) Preservation of near-solar neon isotopic ratios in Icelandic basalts. Earth and Planetary Science Letters, 180, 309–324.

Ellam, R. (1992) Lithospheric thickness as a control on basalt geochemistry. Geology, 20, 153–156.

Farley, Ken A. (1995) Rapid cycling of subducted sediments into the Samoan mantle plume. Geology, 23(6), 531–534.

Farley, Ken A., Natland, Jim H., and Craig, H. (1992) Binary mixing of enriched and undegassed (primitive?) mantle components (He, Sr, Nd, Pb) in Samoan lavas. Earth and Planetary Science Letters, 111, 183–199.

Francis, Don (1985) The Baffin Bay lavas and the value of picrites as analogues of primary magmas. Contributions to Mineralogy and Petrology, 89, 144–154.

Frey, F., Garcia, M., and Roden, M. (1994) Geochemical characteristics of Koolau volcano: Implications of inter-shield geochemical differences among Hawaiian volcanoes. Geochimica et Cosmochimica Acta, 58, 1441–1462.

Füri, E., Hilton, D., Halldørsson, S., Barry, P., Hahm, D., Fischer, T., and Grönvold, K. (2010) Apparent decoupling of the He and Ne isotope systematics of the Icelandic mantle: the role of He depletion, melt mixing, degassing fractionation and air interaction. Geochimica et Cosmochimica Acta, 74(11), 3307–3332.

Gale, Allison, Dalton, Colleen A., Langmuir, Charles H., Su, Y., and Schilling J.G. (2013) The mean composition of ocean ridge basalts. Geochemistry, Geophysics, Geosystems, 14(3), 489-518, doi:10.1029/2012GC004334.

Garcia, M., Hulsebosch, T., and Rhodes, J. (1995) Olivine-rich submarine basalts from the southwest rift zone of Mauna Loa volcano: Implications for magmatic processes and geochemical evolution. In: Rhodes J, Lockwood J, editors. Mauna Loa Revealed: Structure, Composition, History, and Hazards, Geophysics Monograph Series. AGU, 92, 219–39.

Garcia, M.O., Caplan-Auerbach, J., Carlo, E.H.D., Kurz, M.D., and Becker, N. (2006) Geology, geochemistry and earthquake history of Lō'ihi Seamount, Hawai'i's youngest volcano. Chemie der Erde Geochemistry, 66, 81–108, doi:10.1016/j.chemer.2005.09.002.

Garcia, M.O., Hanano, D., Flinders, A., Weis, D., Ito, G., and Kurz, M.D. (2012) Age, geology, geophysics, and geochemistry of Mahukona Volcano, Hawai'i. Bulletin of Volcanology, 74, 1445-1463, doi:10.1007/s00445–012.

Garnero, E.J. and McNamarra, A.K. (2008) Structure and Dynamics of Earth's Lower Mantle. Science, 320(5876), 626-628, doi:10.1126/science.1148028

Geiss, J., Bühler, F., Cerutti, H., Eberhardt, P., Filleux, C., Meister, J., and Signer, P. (2004) The Apollo SWC experiment: Results, conclusions, consequences. Space Science Review, 110, 307–335.

Geist, D.J., Fornari, D.J., Kurz, M.D., Harpp, K.S., Soule, S.A., Perfit, M.R., and Koleszar, A.M. (2006) Submarine Fernandina: Magmatism at the leading edge of the Galápagos hot spot. Geochemistry, Geophysics, Geosystems, 7(12), Q12007, doi:10.1029/2006GC001290.

Gerbode, C., and Dasgupta, R. (2010) Carbonate-fluxed melting of MORB-like pyroxenite at 2.9 GPa and genesis of HIMU ocean island basalts. Journal of Petrology, 51(10), 2067-2088, doi:10.1093/petrology/egq049.

Gonnermann, H.M., and Mukhopadhyay, S. (2009) Preserving noble gases in a convecting mantle. Nature, 459, 560-563, doi:10.1038/nature08018.

Graham, D., Larsen, L., Hanan, B., Storey, M., Pedersen, A., and Lupton, J. (1998) Helium isotope composition of the early Iceland mantle plume inferred from the tertiary picrites of West Greenland. Earth and Planetary Science Letters, 160(3-4), 241–255.

Graham, D.W. (2002) Noble gas isotope geochemistry of mid-ocean ridge and ocean island basalts: Characterization of mantle source reservoirs. In: D. Porcelli CJB, Wieler R, editors. Reviews in Mineralogy and Geochemistry: Noble Gases in Geochemistry and Cosmochemistry. Mineralogiocal Society of America, 47, 247–319.

Graham, D.W., Christie, D.M., Harpp, K.S., and Lupton, J.E. (1993) Mantle plume Helium in submarine basalts from the Galápagos platform. Science, 262, 2023–2026.

Haase, K.M. (1996) The relationship between the age of the lithosphere and the composition of oceanic magmas: Constraints on partial melting, mantle sources and the thermal structure of the plates. Earth and Planetary Science Letters, 144, 75–92.

Hanan, B.B., and Graham D.W. (1996) Lead and Helium isotope evidence from oceanic basalts for a common deep source of mantle plumes. Science, 272(5264), 991-995, doi:10.1126/science.272.5264.991.

Harlou, R. (2007) Understanding magma genesis through analysis of melt inclusions: Application of innovative micro-sampling techniques. Ph.D. thesis; Durham University.

Hart, S.R. (1984) A large scale isotope anomaly in the southern hemisphere mantle. Nature, 309, 753–757.

Hart, S.R., Hauri, E.H., Oschmann, L.A., and Whitehead, J.A. (1992) Mantle plumes and entrainment: Isotopic evidence. Science, 256(5056), 517-520, doi:10.1126/science.256.5056.517.

Hart, S.R., and Jackson, M.G. (2014) Ta'u and Ofu/Olosega volcanoes: The "Twin Sisters" of Samoa, their P, T, X melting regime, and global implications. Geochemistry, Geophysics, Geosystems, 15(6), 2301-2318, doi:10.1002/ 2013GC005221.

Hauri, E.H. (1996) Major-element variability in the Hawaiian mantle plume. Nature, 382, 415–419.

Herzberg, C. (2010) Identification of source lithology in the Hawaiian and Canary islands: Implications for origins. Journal of Petrology, 52(1), 113-146, doi:10.1093/petrology/egq075

Hilton, D.R., Grönvold, K., Macpherson, C.G., and Castillo P.R. (1999) Extreme $^{3}He/^{4}He$ ratios in northwest Iceland: constraining the common component in mantle plumes. Earth and Planetary Science Letters, 173, 53–60.

Hirose, K., and Kushiro, I. (1993) Partial melting of dry peridotites at high pressures: Determination of compositions of melts segregated from peridotite using aggregates of diamond. Earth and Planetary Science Letters, 114(4), 477-489, doi:10.1016/0012–821X(93)90077.

Hofmann, A.W. (1997) Mantle geochemistry: the message from oceanic volcanism. Nature, 385, 226–229.

Hofmann, A.W., and White, W.M. (1982) Mantle plumes from ancient oceanic crust. Earth and Planetary Science Letters, 57, 421–436.

Huang, S., Farkas, J., and Jacobsen, S. (2011) Stable calcium isotopic compositions of Hawaiian shield lavas: Evidence for recycling ancient marine carbonates into the mantle. Geochimica et Cosmochimica Acta, 75, 4987-4997, doi:10.1016/j.gca.2011.06.010.

959 Huang, S., and Frey, F.A. (2005) Recycled oceanic crust in the Hawaiian plume:
960 Evidence from temporal geochemical variations within the Koolau shield. Contributions
961 to Mineralogy and Petrology, 149, 556–575.

962 Huang, S., Frey, F.A., Blichert-Toft, J., Fodor, R., Bauer, G., and Xu, G. (2005) Enriched
963 components in the Hawaiian plume: Evidence from Kahoolawe volcano, Hawai'i.
964 Geochemistry, Geophysics, Geosystems, 6, Q11006, doi:10.1029/2005GC001012.

965 Huang, S., Humayun, M., and Frey, F.A. (2007) Iron/ Manganese ratio and Manganese
966 content in shield lavas from Ko'olau volcano, Hawai'i. Geochimica et Cosmochimica
967 Acta, 71, 4557-4569, doi:10.1016/j.gca.2007.07.013.

968 Huang, S., Jacobsen, and S.B., Mukhopadhyay, S. (2013) ^{147}Sm-^{143}Nd systematics of
969 Earth are inconsistent with a superchondritic Sm/Nd ratio. PNAS, 110(13), 4929–4934.

970 Ito, Garrett and Mahoney, J. J. (2005) Flow and melting of a heterogeneous mantle: 1.
971 Method and importance to the geochemistry of ocean island and mid-ocean ridge basalts.
972 Earth and Planetary Science Letters, 230, 29–46, doi:10.1016/j.epsl.2004.10.035.

973 Jackson, M.G., and Carlson, R.W. (2011) An ancient recipe for flood-basalt genesis.
974 Nature, 476, 316–319, doi:10.1038/nature10326.

975 Jackson, M.G., and Carlson, R.W. (2012) Homogeneous superchondritic ^{142}Nd/^{144}Nd in
976 the mid-ocean ridge basalt and ocean island basalt mantle. Geochemistry, Geophysics,
977 Geosystems, 13(6), Q06011doi:10.1029/2012GC004114.

978 Jackson, M.G., Carlson, R.W., Kurz, M.D., Kempton, P.D., Francis, D., and Blusztajn,
979 J.S. (2010) Evidence for the survival of the oldest terrestrial mantle reservoir. Nature, 466,
980 853-856, doi:10.1038/nature09287.

981 Jackson, M.G., and Dasgupta, R. (2008) Compositions of HIMU, EM1, and EM2 from
982 global trends between radiogenic isotopes and major elements in ocean island basalts.
983 Earth and Planetary Science Letters, 276, 175–186.

984 Jackson, M.G., Hart, S.R., Saal, A.E., Shimizu, N., Kurz, M.D., Blusztajn, J.S., and
985 Skovgaard, A.C. (2008) Globally elevated Titanium, Tantalum, and Niobium (TITAN) in

ocean island basalts with high $^{3}He/^{4}He$. Geochemistry, Geophysics, Geosystems, 9(4), Q04027, doi:10.1029/2007GC001876.

Jackson, M.G., and Jellinek, A. (2013) Major and trace element composition of the high $^{3}He/^{4}He$ mantle: Implications for the composition of the bulk silicate Earth. Geochemistry, Geophysics, Geosystems, 2954–2976, 14(8), 2954-2976, doi:10.1002/ggge.20188.

Jackson, M.G., Kurz, M.D., and Hart, S.R. (2009) Helium and Neon isotopes in phenocrysts from Samoan lavas: Evidence for heterogeneity in the terrestrial high $^{3}He/^{4}He$ mantle. Earth and Planetary Science Letters, 287, 519–528.

Jackson, M.G., Kurz, M.D., Hart, S.R., and Workman, R.K. (2007) New Samoan lavas from Ofu island reveal a hemispherically heterogeneous high $^{3}He/^{4}He$ mantle. Earth and Planetary Science Letters, 264, 360–374.

Jackson, M.G., Weis, D., and Huang, S. (2012) Major element variations in Hawaiian shield lavas: Source features and perspectives from global ocean is land basalt (OIB) systematics. Geochemistry, Geophysics, Geosystems, 13(9), Q09009, doi:10.1029/2012GC004268.

Keller, R.A., Graham, D.W., Farley, K.A., Duncan, R.A., and Lupton, J.E. (2004) Cretaceous-to-recent record of elevated $^{3}He/^{4}He$ along the Hawaiian- Emperor volcanic chain. Geochemistry, Geophysics, Geosystems, 5(12), Q12L05, doi:10.1029/2004GC000739.

Kent, A., Stopler, E., Francis, D., Woodhead, J., Frei, R., and Eiler, J. (2004) Mantle heterogeneity during the formation of the North Atlantic igneous province: Constraints from trace element and Sr-Nd-Os-O isotope systematics of Baffin Island picrites. Geochemistry, Geophysics, Geosystems, 5, Q11004, doi:10.1029/2004GC000743.

Kessel, R., Schmidt, M.W., Ulmer, P., and Pettke, T. (2005) Trace element signature of subduction-zone fluids, melts and supercritical liquids at 120-180 km depth. Nature, 437, 724-727, doi:10.1038/nature03971.

Kinoshita, N., Paul, M., Kashiv, Y., Collon, P., Deibel, C., DiGiovine, B., Greene, J., Henderson, D., Jiang, C., Marley, S., Nakanashi, T., Pardo, R., Rehm, K., Robertson, D., Scott, R., Schmidt, C., Tang, X., Vondrasek, R., and Yokoyama, A. (2012) A shorter ^{146}Sm half-life measured and implications for ^{146}Sm-^{142}Nd chronology in the solar system. Science, 335(6076), 1614–1617.

Koppers, A.A.P., Russell, J.A., Roberts, J., Jackson, M.G., Konter, J.G., Wright, D.J., Staudigel, H., and Hart, S.R. (2011) Age systematics of two young en echelon Samoan volcanic trails. Geochemistry, Geophysics, Geosystems, 12(7), Q07025, doi:10.1029/2010GC003438.

Kurz, M.D., Jenkins, W., Hart, S.R. (1982) Helium isotopic systematics of oceanic islands and mantle heterogeneity. Nature, 297, 43–47.

Kurz, M.D., Curtice, J., Fornari, D., Geist, D., and Moreira, M. (2009) Primitive neon from the center of the Galápagos hotspot. Earth and Planetary Science Letters, 286 (1-2), 23-34, doi:10.1016/j.epsl.2009.06.008.

Kurz, M.D., and Geist, D. (1999) Dynamics of the Galapagos hotspot from helium isotope geochemistry. Geochimica et Cosmochimica Acta, 63(23/24), 4139–4156.

Kurz, M.D., Jenkins, W.J., Hart, S.R., Kurz, M.D., Jenkins, W.J., Hart, S.R., and Clague, D. Helium isotopic variations in volcanic rocks from Loihi seamount and the island of Hawaii. Earth and Planetary Science Letters, 66, 388-406, doi:10.1016/0012–821X(83)90154.

Kurz, M.D., Meyer, P.S., and Sigurdsson, H. (1985) Helium isotopic systematics within the neovolcanic zones of Iceland. Earth and Planetary Science Letters, 74, 291–305.

Labrosse, S., Hernlund, J.W., and Coltice, N. (2007) A crystallizing dense magma ocean at the base of the Earth's mantle. Nature, 450, 866-869, doi:10.1038/nature06355.

Langmuir, C., Klein, E., and Plank, T. (1992) Petrological systematics of mid-ocean ridge basalts: Constraints on melt generation beneath ocean ridges. In: Morgan J, editor.

Mantle flow and melt generation at mid-ocean ridges: American Geophysical Union Geophysical Monograph. AGU Monograph, 71, 183–280.

Larsen, L.M., and Pedersen, A.K. (2009) Petrology of the paleocene picrites and flood basalts on Disko and Nuussuaq, West Greenland. Journal of Petrology, 50(9), 1667-1711, doi:10.1093/petrology/egp048.

Lee, C.T.A., Luffi, P., Höink, T., Li, J., Dasgupta, R., and Hernlund, J. (2010) Upside-down differentiation and generation of a 'primordial' lower mantle. Nature, 463, 930-933, doi:10.1038/nature08824.

Lee, C.T.A., Luffi, P., Plank, T., Dalton, H., and Leeman, W.P. (2009) Constraints on the depths and temperatures of basaltic magma generation on Earth and other terrestrial planets using new thermobarometers for mafic magmas. Earth and Planetary Science Letters, 279, 20–33.

Li, M., McNamara, A.K., and Garnero, E.J. (2014) Chemical complexity of hotspots caused by cycling oceanic crust through mantle reservoirs. Nature Geoscience, 7, 366-370, doi:10.1038/NGEO2120.

Macdonald, G.A., Katsura, T. (1964) Chemical composition of Hawaiian lavas. Journal of Petrology, 5(1), 82-133, doi:10.1093/petrology/5.1.82.

Macpherson, C.G., Hilton, D.R., Day, J.M.D., Lowry, D., and Grönvold, K. (2005) High-$^{3}He/^{4}He$, depleted mantle and low-$\delta^{18}O$, recycled oceanic lithosphere in the source of central Iceland magmatism. Earth and Planetary Science Letters, 233, 411–427.

Mahaffy, P., Donahue, T., Atreya, S., Owen, T., and Niemann, H. (1998) Galileo probe measurements of D/H and $^{3}He/^{4}He$ in Jupiter's atmosphere. Space Science Reviews, 84, 251–263.

Mallik, A., and Dasgupta, R. (2012) Reaction between MORB-eclogite derived melts and fertile peridotite and generation of ocean island basalts. Earth and Planetary Science Letters, 329–330, 97–108, doi:10.1016/j.epsl.2012.02.007.

Mallik, A., and Dasgupta, R. (2013) Reactive infiltration of MORB-eclogite-derived carbonated silicate melt into fertile peridotite at 3 GPa and genesis of alkalic magmas. Journal of Petrology, 54(11), 2267-2300, doi:10.1093/petrology/egt047.

Mallik, A., and Dasgupta, R. (2014) Effect of variable CO_2 on eclogite-derived andesite and lherzolite reaction at 3 GPa-Implications for mantle source characteristics of alkalic ocean island basalts. Geochemistry, Geophysics, Geosystems, 15(4), 1533-1557, doi:10.1002/2014GC005251.

McDonough, W., and Sun, S. (1995) The composition of the Earth. Chemical Geology, 120, 223–253.

McDougall, I. (2010) Age of volcanism and its migration in the Samoa islands. Geological Magazine, 147, 705-717, doi:10.1017/S0016756810000038.

McKenzie, D., and O'Nions, R. (1991) Partial Melt Distributions from Inversion of Rare Earth Element Concentrations. Journal of Petrology, 32(5), 1021-1091, doi: 10.1093/petrology/32.5.1021.

Melson, W.G., O'Hearn, T., and Jarosewich, E. (2002) A data brief on the Smithsonian Abyssal Volcanic Glass Data File. Geochemistry, Geophysics, Geosystems, 3(4), 1-11, doi:10.1029/2001GC000249.

Moreira, M., Breddam, C., Curtice, J., and Kurz, M.D. (2001) Solar Neon in the Icelandic mantle: Evidence for an undegassed lower mantle. Earth and Planetary Science Letters, 185, 15–23.

Morgan, W.J. (1971) Convection plumes in the lower mantle. Nature, 230, 42 – 43, doi:10.1038/230042a0.

Mukhopadhyay, S. (2012) Early differentiation and volatile accretion recorded in deep-mantle Neon and Xenon. Nature, 486, 101–104, doi:10.1038/nature11141.

Mukhopadhyay, S., Lassiter, J.C., Farley, K.A., and Bogue, S.W. (2003) Geochemistry of Kauai shield-stage lavas: Implications for the chemical evolution of the Hawaiian plume. Geochemistry, Geophysics, Geosystems, 4(1), 1009, doi:10.1029/2002GC000342.

Panning, M., and Romanowicz, B. (2006) A three-dimensional radially anisotropic model of shear velocity in the whole mantle. Geophysical Journal International, 167(1), 361–379.

Parai, R., Mukhopadhyay, S., and Lassiter, J.C. (2009) New constraints on the HIMU mantle from Neon and Helium isotopic compositions of basalts from the Cook-Austral Islands. Earth and Planetary Science Letters, 277, 253–261.

Parman, S.W. (2007) Helium isotopic evidence for episodic mantle melting and crustal growth. Nature, 446, 900–903, doi:10.1038/nature05691.

Parman, S.W., Kurz, M.D., Hart, S.R., and Grove, T.L. (2005) Helium solubility in olivine and implications for high $^{3}He/^{4}He$ in ocean island basalts. Nature, 437, 1140-1143, doi:10.1038/nature04215.

Perfit, M., Fornari, D., Ridley, W., Kirk, P., Casey, J., Kastens, K., Reynolds, J., Edwards, M., Shuster, R., and Paradis, S. (1996) Recent volcanism in the Siqueiros transform fault: picritic basalts and implications for MORB magma genesis. Earth and Planetary Science Letters, 141, 91–108.

Petermann, M., and Hirschmann, M.M. (2003) Anhydrous partial melting experiments on a MORB-like eclogite: phase relations, phase compositions and mineral- melt partitioning of major elements at 2-3 GPa. Journal of Petrology, 44, 2173–2201.

Petö, M.K., Mukhopadhyay, S., and Kelley, K.A. (2013) Heterogeneities from the first 100 million years recorded in deep heterogeneities from the first 100 million years recorded in deep mantle noble gases from the northern Lau back-arc basin. Earth and Planetary Science Letters, 369-370, 13–23.

Prytulak, J., and Elliot, T. (2007) TiO_2 enrichment in ocean island basalts. Earth and Planetary Science Letters, 263, 388–403.

Putirka, K. (2008) Excess temperatures at ocean islands: Implications for mantle layering and convection. Geology 2008, 36(4), 283-286, doi:10.1130/G24615A.1.

Qin, L., Carlson, R.W., and Alexander, C.M. (2011) Correlated nucleosynthetic isotopic variability in Cr, Sr, Ba, Sm, Nd and Hf in Murchison and QUE 97008. Geochimica et Cosmochimica Acta, 75(24), 7806–7828.

Ranen, M.C., and Jacobsen, S.B. (2006) Barium Isotopes in Chondritic Meteorites: Implications for Planetary Reservoir Models. Science, 314, 809–812.

Rison, W., and Craig, H. (1983) Helium isotopes and mantle volatiles in Loihi seamount and Hawaiian island baslats and xenoliths. Earth and Planetary Science Letters, 66, 407–426.

Robillard, I., Francis, D., and Ludden, J. (1992) The relationship between E- and N-type magmas in the Baffin Bay lavas. Contributions to Mineralogy and Petrology, 112, 230–241.

Saunders, A., Fitton, J., Kerr, A., Norry, M., and Kent, R. (1997) The North Atlantic igneous province. In: Mahoney J, Coffin M, editors. Large Igneous Provinces: Continental, Oceanic and Planetary Volcanism. AGU Monograph, 100, 45–94.

Sobolev, A.V., Hofmann, A.W., Sobolev, S.V., and Nikogosian, I.K. (2005) An olivine-free mantle source of Hawaiian shield basalts. Nature, 434, 590–597.

Spandler, C., Yaxley, G., Green, D., and Rosenthal, A. (2008) Phase relations and melting of anhydrous K-bearing eclogite from 1200 to to 1600^{o}C and 3 to 5 GPa. Journal of Petrology, 49(4), 771-795, doi:10.1093/petrology/egm039.

Sprung, P., Kleine, T., and Scherer, E.E. (2013) Isotopic evidence for chondritic Lu/Hf and Sm/Nd of the Moon. Earth and Planetary Science Letters, 380, 77–87.

Starkey, N.A., Stuart, F.M., Ellam, R.M., Fitton, J.G., Basu, S., and Larsen, L.M. (2009) Helium isotopes in early Iceland plume picrites: Constraints on the composition of high ^{3}He/^{4}He mantle. Earth and Planetary Science Letters, 277, 91–100, doi:10.1016/j.epsl.2008.10.007.

Staudacher, T., and Allègre, C.J. (1988) Recycling of oceanic crust and sediments: the noble gas subduction barrier. Earth and Planetary Science Letters, 89, 173–183.

1145 Stracke, A., Hofmann, A.W., Hart, S.R. (2005) FOZO, HIMU, and the rest of the mantle
1146 zoo. Geochemistry, Geophysics, Geosystems, 6(5), Q05007, doi:10.1029/2004GC000824.

1147 Stuart, F., Lass-Evans, S., Fitton, J., and Ellam, R.M. (2003) High $^{3}He/^{4}He$ ratios in
1148 picritic basalts from Baffin Island and the role of a mixed reservoir in mantle plumes.
1149 Nature, 424, 57–59.

1150 Takahashi, E. (1986) Melting of a dry peridotite KLB-1 up to 14 GPa: Implications on
1151 the origin of peridotitic upper mantle. Journal of Geophysical Research, 91(10), 9367-
1152 9382, doi:10.1029/JB091iB09p09367.

1153 Tamura, Y., Yuhara, M., Ishii, T. (2000) Primary arc basalts from Daisen Volcano,
1154 Japan: equilibrium crystal fractionation versus disequilibrium fractionation during
1155 supercooling. Journal of Petrology, 41, 431–448.

1156 Torsvik, T.H., Burke, K., Steinberger, B., Webb, S.J., and Ashwal, L.D. (2010)
1157 Diamonds sampled by plumes from the core-mantle boundary. Nature, 466, 352–355.

1158 Tucker, J., and Mukhopadhyay, S. (2014) Evidence for multiple magma ocean outgassing
1159 and atmospheric loss episodes from mantle noble gases. Earth and Planetary Science
1160 Letters, 393, 254–265.

1161 Valbracht, P.J., Staudacher, T., Malahoff, A., and Allègre, C.J. (1997) Noble gas
1162 systematics of deep rift zone glasses from Loihi Seamount, Hawaii. Earth and Planetary
1163 Science Letters, 150, 399–411.

1164 Walter, M. (1998) Melting of garnet peridotite and the origin of komatiite and depleted
1165 lithosphere. Journal of Petrology, 36(1), 29-60, doi:10.1093/petroj/39.1.29.

1166 Watson, S., and McKenzie, D. (1991) Melt generation by plumes: a study of Hawaiian
1167 volcanism. Journal of Petrology, 32, 501–537.

1168 Workman, R.K., Hart, S.R., Jackson, M.G., Regelous, M., Farley, K.A., Blusztajn, J.,
1169 Kurz, M.D., and Staudigel, H. (2004) Recycled metasomatized lithosphere as the origin
1170 of the Enriched Mantle II (EM2) end-member: Evidence from the Samoan volcanic chain.
1171 Geochemistry, Geophysics, Geosystems, 5(4), Q04008, doi: 10.1029/2003GC000623.

1172 Yasuda, A., Fujii, T., and Kurita, K. (1994) Melting phase relations of an anhydrous mid-
1173 ocean ridge basalt from 3 to 20 GPa: implications for the behavior of subducted oceanic
1174 crust in the mantle. Journal of Geophysical Research, 99(B5), 9401–9414,
1175 doi: 10.1029/93JB03205

1176 Zindler, A., and Hart, S.R. (1986) Chemical geodynamics. Ann Rev Earth Planet Sci, 14,
1177 493–571.

1178 Zindler, A., Jagoutz, E., and Goldstein, S.L. (1982) Nd, Sr and Pb isotopic systematics in
1179 a three-component mantle: a new perspective. Nature, 298, 519–523.

1180

Figure captions

Figure 1: Map with the locations of high $^3He/^4He$ lavas discussed in this study. The map also shows seismic shear wave velocity anomalies at 2,800 km depth from the SAW642AN model (Panning and Romanowicz, 2006).

Figure 2: MgO vs. other major element oxides of the global OIBs (from Jackson and Dasgupta, 2008) and high $^3He/^4He$ lavas. MORBs are shown for reference. The data are normalized to 100 wt.% on a dry basis. The data in this figure and in all the following figures that display geochemical relationships are divided into several categories based on the respective geochemical characteristics, and these categories are displayed in the figure legend. High $^3He/^4He$ lavas encompass a wide range of major element compositions. The total alkali vs. silica classification (TAS) is from Macdonald and Katsura (1964). Hotspots with carbonatite flows and dikes−the Cape Verde and Canary hotspots−anchor extreme compositions that are not observed in the highest $^3He/^4He$ lavas. Among the BIWG lavas, data for BIWG from Starkey et al. (2009) are shown separately, as these lavas do not have Pb-isotopic compositions required for evaluating crustal assimilation. TiO_2 and Na_2O are plotted on logarithmic scale.

Figure 3: Olivine fractionation corrected major element compositions of the global OIBs (from Jackson and Dasgupta, 2008) and high $^3He/^4He$ lavas. MORBs are shown for reference. High $^3He/^4He$ lavas lavas do not extend to the extreme compositions (with low SiO_2 and high CaO/Al_2O_3) found in hotspots with carbonatites (Cape Verde and Canary Islands) and the high SiO_2 and high FeO compositions found in Hawaii Koolau lavas. However, some high $^3He/^4He$ lavas such as those from Ofu and Loihi have high TiO_2, SiO_2 well below 45 wt. %, and $FeO_T > 11$ wt. %. Only high $^3He/^4He$ lavas with MgO > 8 wt. % are shown, except for Ofu, where lavas with > 10 wt. % MgO are shown. All lava compositions are corrected to be in equilibrium with olivine of Fo_{90}. Pressure vectors are qualitative.

Figure 4: Radiogenic isotopic compositions in $^3He/^4He$ lavas indicate source heterogeneity. All high $^3He/^4He$ lavas, except BIWG, are shifted to the right of the 4.5-Ga geochron in Pb-isotopic space which suggests a presence of recycled material mixed into high $^3He/^4He$ reservoir at all locations (except for possibly BIWG). The high $^3He/^4He$

lavas sampled by ocean island basalts also exhibit $^{143}Nd/^{144}Nd$ compositions higher than chondrite, suggesting a history of long-term incompatible element depletion of high $^{3}He/^{4}He$ reservoir. The NHRL (Northern Hemisphere Reference Line) is from Hart (1984).

Figure 5: $^{206}Pb/^{204}Pb$ vs. olivine-fractionation corrected SiO_2, TiO_2 and CaO/Al_2O_3 of global OIBs (from Jackson and Dasgupta, 2008) and high $^{3}He/^{4}He$ lavas. Lavas with high $^{3}He/^{4}He$ span a wide range of major element and isotopic compositions. The MORB field is shown as light-grey rectangle: the isotopic compositions for MORB are from Gale et al. (2013), and the major element composition of MORB is from Figure 4. TiO_2 tends to increase with increasing $^{206}Pb/^{204}Pb$. Only high $^{3}He/^{4}He$ lavas with MgO > 8 wt.% are shown, except for Ofu, where lavas with > 10% MgO are shown. Due to the scarcity of paired major element and isotopic data for samples with MgO > 8 wt.% from Fernandina, Fernandina is also shown as a field that presents all olivine- fractionation-corrected lavas with high MgO (MgO > 8 wt. %) (from Figure 3) and all available $^{206}Pb/^{204}Pb$ ratios from the island. All lava compositions are corrected to be in equilibrium with olivine of Fo_{90}.

Figure 6: A schematic representation of the effects of LAB thickness on melting pyroxenite/eclogite vs. peridotite. Melts generated at higher pressures (such as melts beneath Ofu and Loihi) will exhibit a pronounced mafic (pyroxenite/eclogite) component and volatile (specifically CO_2 in the source) signature. At shallower pressures, the signature of a mafic component and mantle CO_2 will be diluted owing to a greater proportion of volatile-free peridotite melting. The figure is modified after Prytulak and Elliot (2007) and Dasgupta et al. (2010).

Figure 7: TiO_2 variability in global OIBs and high $^{3}He/^{4}He$ lavas. a. Average TiO_2 concentrations are plotted against the depth of the lithosphere-asthenosphere boundary (LAB) at the time of volcanism: LAB depths and island-averaged TiO_2 compositions are taken from Dasgupta et al. (2010) (grey symbols). Averages for $^{3}He/^{4}He$ localities are calculated in this study. For BIWG, the LAB depth for Iceland is used. The horizontal lines show TiO_2 concentrations that can be obtained by melting of primitive peridotite (McDonough and Sun, 1995) using the Prytulak and Elliot (2007) melt model at the following degrees of melting in the garnet and spinel stability fields: 0% melt (solid lines)

and 5% melt (dashed lines), in garnet stability field (red lines) and spinel stability field (black lines). b. A relationship between calculated pressures of melting and concentrations of TiO_2 in global OIBs and high $^3He/^4He$ lavas. The pressures were calculated from major element compositions using the parametrization of Lee et al. (2009), and only lavas with $SiO_2 > 44$ wt.% are shown, as the barometer is not calibrated for highly silica-undersaturated lavas. c. Reference TiO_2 concentration for each of the island groups (all grey symbols) are taken from Prytulak and Elliot (2007). Reference TiO_2 concentrations for high $^3He/^4He$ lavas are calculated using the method outlined for each island group in Prytulak and Elliot (2007). Lines show TiO_2 concentrations are the same as in panel a.

Figure 8: SiO_2 vs. TiO_2, Al_2O_3, FeO_T , CaO, Na_2O and CaO/Al_2O_3 of high $^3He/^4He$ lavas from Baffin Island, Iceland, Fernandina, Loihi (alkalic and tholeiitic lavas) and Ofu. The lavas have been corrected to be in equilibrium with Fo_{88} olivine (the average Mg# of olivines in eclogite-melt hybridization of peridotite according to Mallik and Dasgupta, 2012, 2013, 2014). Also plotted in the figure are fields representing composition of volatile-free peridotite partial melts generated between 2-4 GPa with degree of partial melting up to 20 % (Walter, 1998; Hirose and Kushiro, 1993; Takahashi, 1986; Davis et al., 2011) and curves of modeled isopleths of eclogite-melt peridotite hybridization is from Mallik and Dasgupta (2014). The solid and dashed curves are isopleths of eclogite-melt fraction from 0 to 35 wt.% and amount of CO_2 in the eclogite-melt peridotite hybridization (from 0 to 2 wt.%), respectively. The dashed black lines represent dry-peridotite partial melt field. In order to best match the average compositions of the alkalic lavas from Ofu and Loihi with the model, the reacted melt from eclogite-melt hybridization with peridotite has to undergo a second stage mixing with volatile-free peridotite partial melt (see text for details).

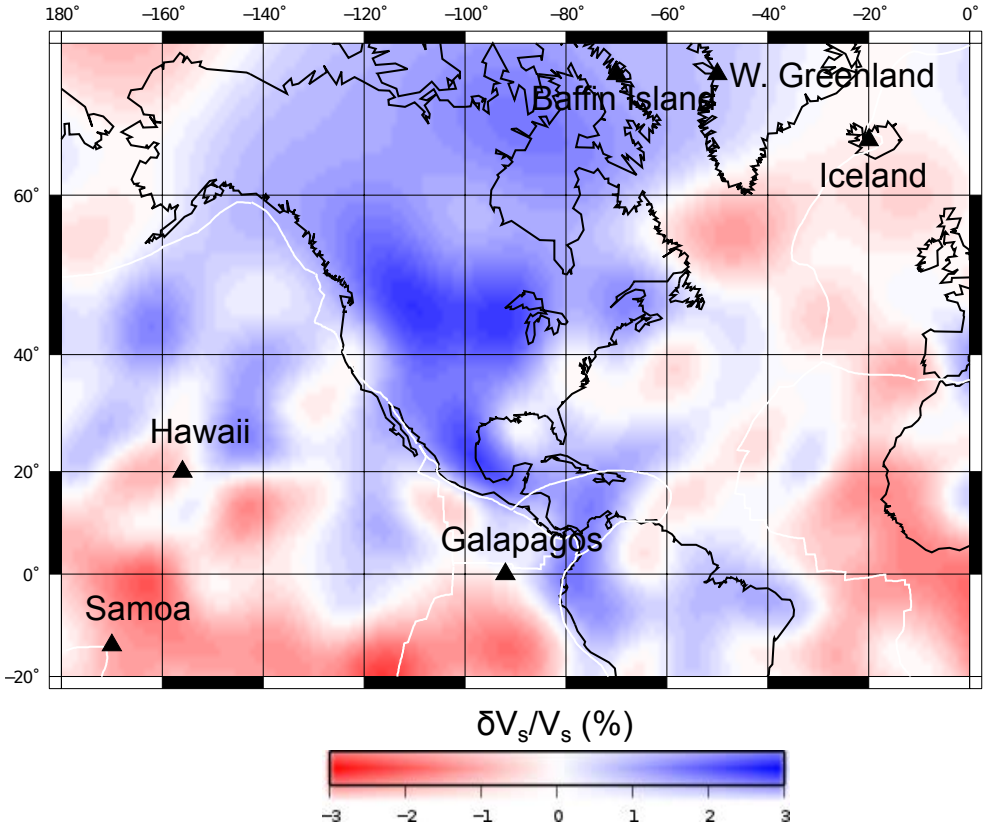

Figure 1: Map with the locations of high $^{3}He/^{4}He$ lavas discussed in this study. The map also shows seismic shear wave velocity anomalies at 2,800 km depth from the SAW642AN model (Panning and Romanowicz, 2006).

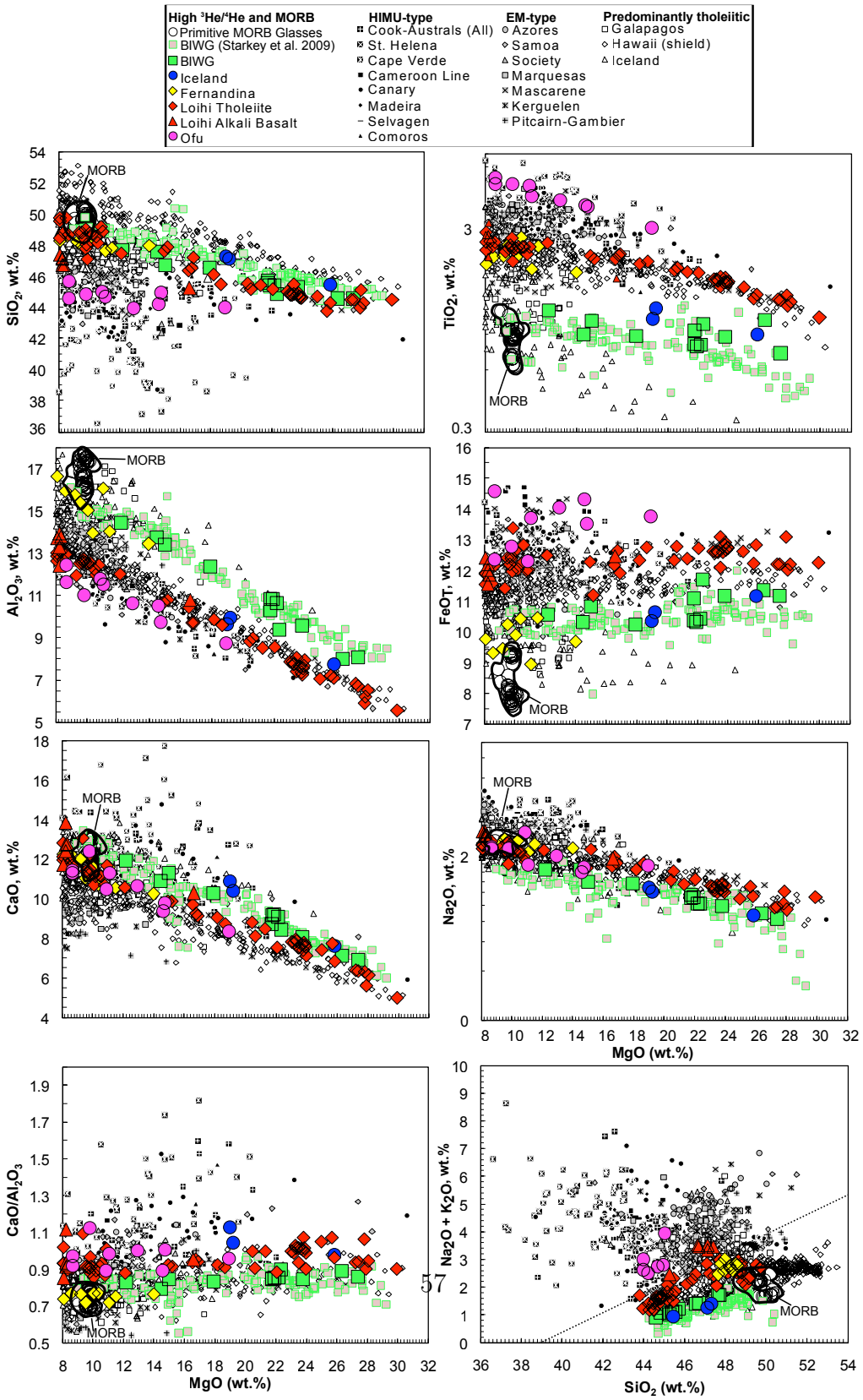

Figure 2

MgO vs. other major element oxides of the global OIBs (from Jackson and Dasgupta, 2008) and high $^3He/^4He$ lavas. MORBs are shown for reference. The data are normalized to 100 wt.% on a dry basis. The data in this figure and in all the following figures that display geochemical relationships are divided into several categories based on the respective geochemical characteristics, and these categories are displayed in the figure legend. High $^3He/^4He$ lavas encompass a wide range of major element compositions. The total alkali vs. silica classification (TAS) is from Macdonald and Katsura (1964). Hotspots with carbonatite flows and dikes−the Cape Verde and Canary hotspots−anchor extreme compositions that are not observed in the highest $^3He/^4He$ lavas. Among the BIWG lavas, data for BIWG from Starkey et al. (2009) are shown separately, as these lavas do not have Pb-isotopic compositions required for evaluating crustal assimilation. TiO_2 and Na_2O are plotted on logarithmic scale.

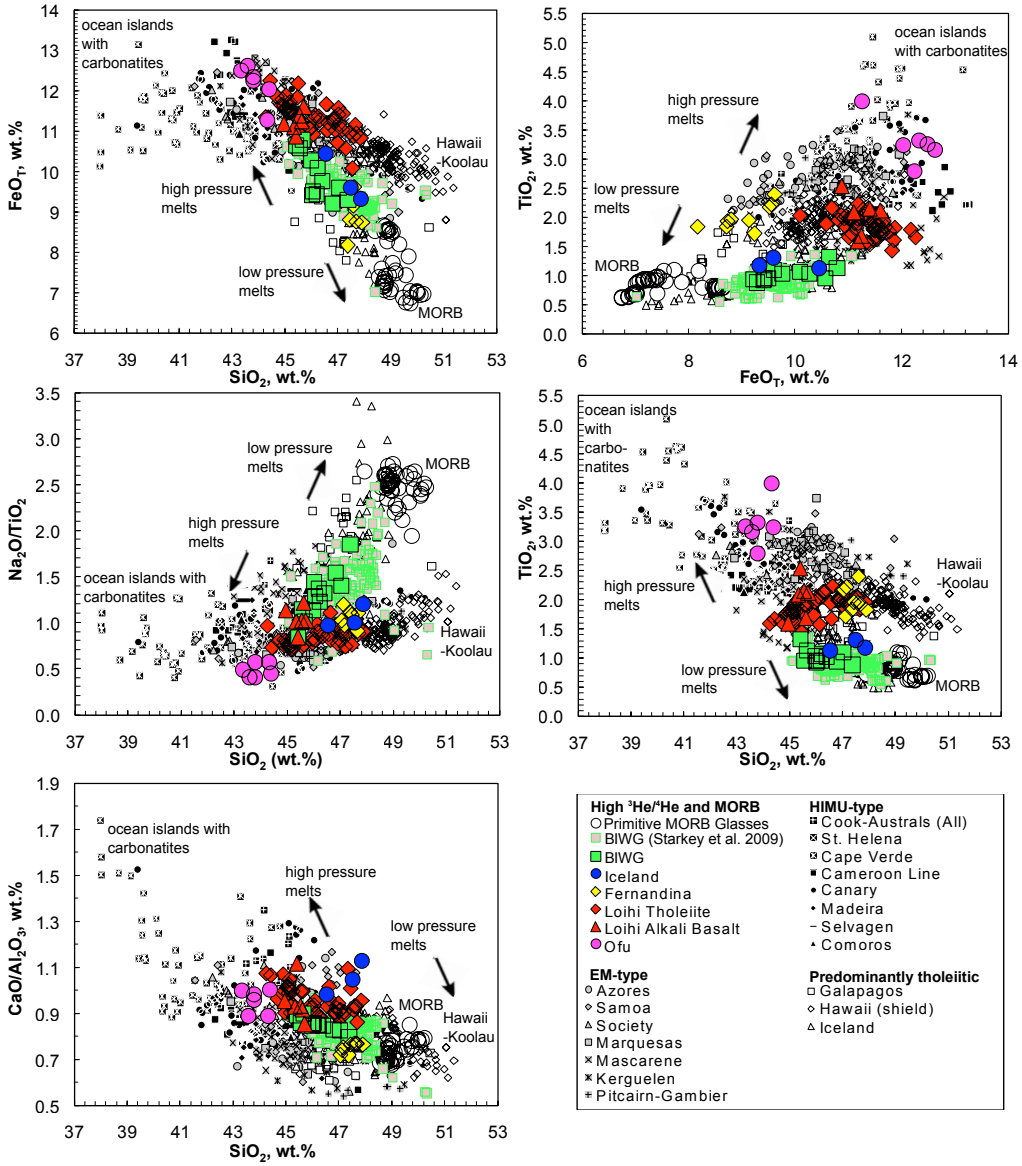

Figure 3

Olivine fractionation corrected major element compositions of the global OIBs (from Jackson and Dasgupta, 2008) and high $^3He/^4He$ lavas. MORBs are shown for reference. High $^3He/^4He$ lavas lavas do not extend to the extreme compositions (with low SiO_2 and high CaO/Al_2O_3) found in hotspots with carbonatites (Cape Verde and Canary Islands) and the high SiO_2 and high FeO compositions found in Hawaii Koolau lavas. However, some high $^3He/^4He$ lavas such as those from Ofu and Loihi have high TiO_2, SiO_2 well below 45 wt. %, and $FeO_T > 11$ wt. %. Only high $^3He/^4He$ lavas with MgO > 8 wt. % are shown, except for Ofu, where lavas with > 10 wt. % MgO are shown. All lava compositions are corrected to be in equilibrium with olivine of Fo_{90}. Pressure vectors are qualitative.

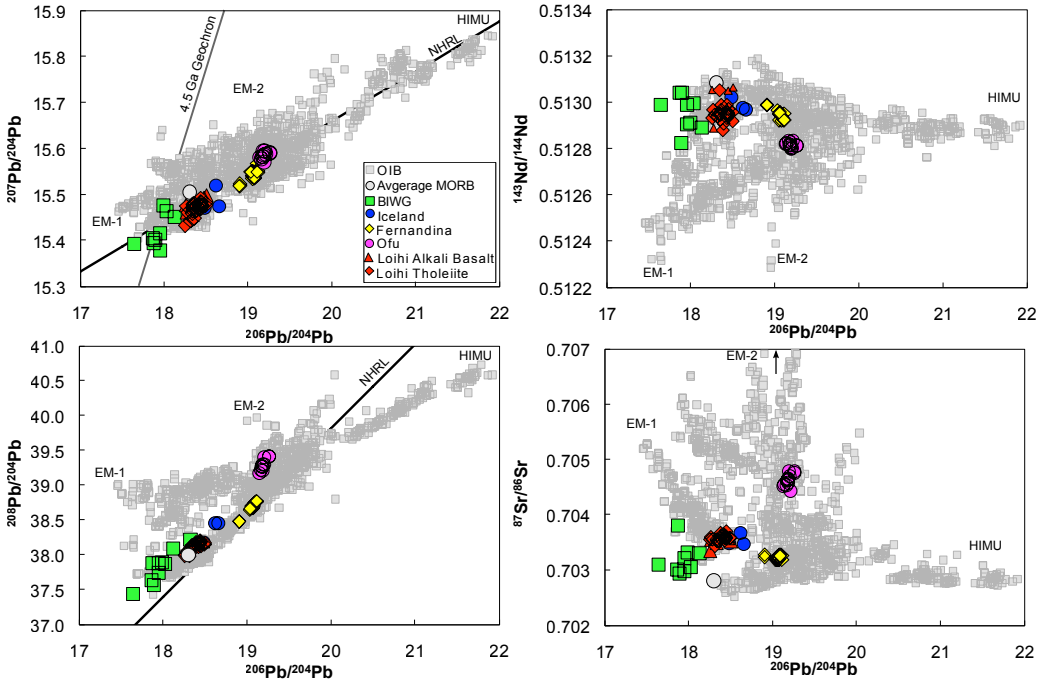

Figure 4: Radiogenic isotopic compositions in $^{3}He/^{4}He$ lavas indicate source heterogeneity. All high $^{3}He/^{4}He$ lavas, except BIWG, are shifted to the right of the 4.5 Ga geochron in Pb-isotopic space which suggests a presence of recycled material mixed into high $^{3}He/^{4}He$ reservoir at all locations (except for possibly BIWG). The high $^{3}He/^{4}He$ lavas sampled by ocean island basalts also exhibit $^{143}Nd/^{144}Nd$ compositions higher than chondrite, suggesting a history of long-term incompatible element depletion of high $^{3}He/^{4}He$ reservoir. The NHRL (Northern Hemisphere Reference Line) is from Hart (1984).

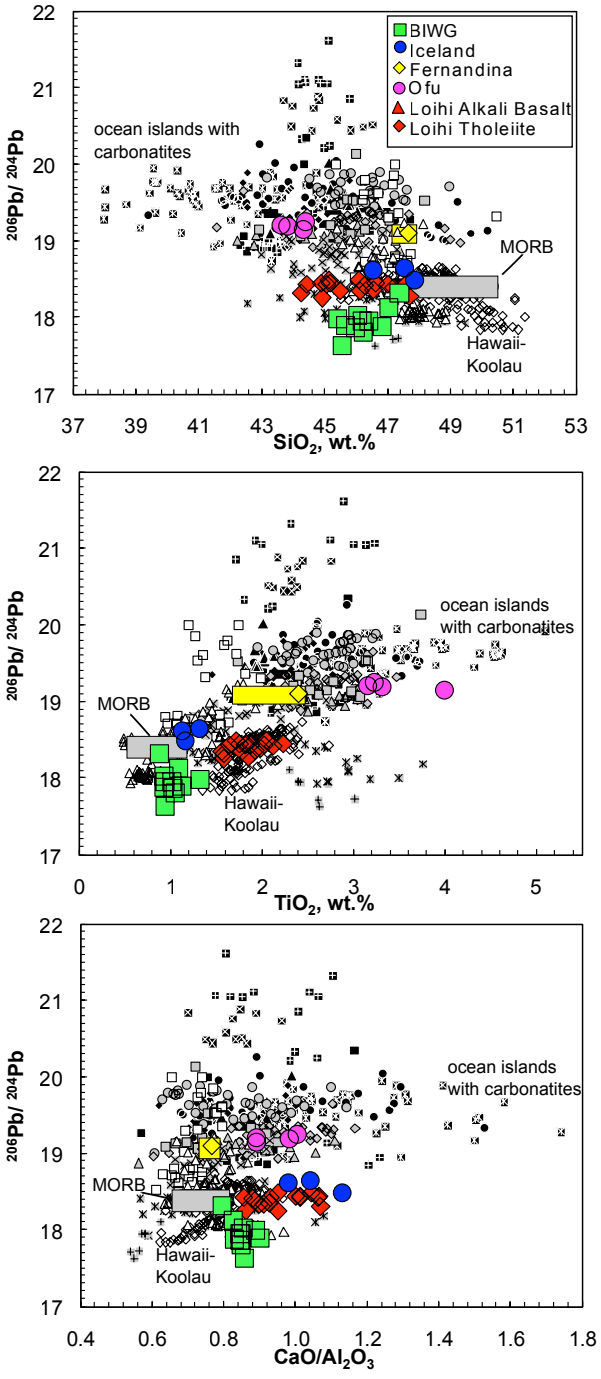

Figure 5

$^{206}Pb/^{204}Pb$ vs. olivine-fractionation corrected SiO_2, TiO_2 and CaO/Al_2O_3 of global OIBs (from Jackson and Dasgupta, 2008) and high $^{3}He/^{4}He$ lavas. Lavas with high $^{3}He/^{4}He$ span a wide range of major element and isotopic compositions. The MORB field is shown as light-grey rectangle: the isotopic compositions for MORB are from Gale et al. (2013), and the major element composition of MORB is from Figure 4. TiO_2 tends to increase with increasing $^{206}Pb/^{204}Pb$. Only high $^{3}He/^{4}He$ lavas with MgO>8 wt.% are shown, except for Ofu, where lavas with $> 10\%$ MgO are shown. Due to the scarcity of paired major element and isotopic data for samples with MgO > 8 wt.% from Fernandina, Fernandina is also shown as a field that presents all olivine-fractionation-corrected lavas with high MgO (MgO > 8 wt. %) (from Figure 3) and all available $^{206}Pb/^{204}Pb$ ratios from the island. All lava compositions are corrected to be in equilibrium with olivine of Fo_{90}.

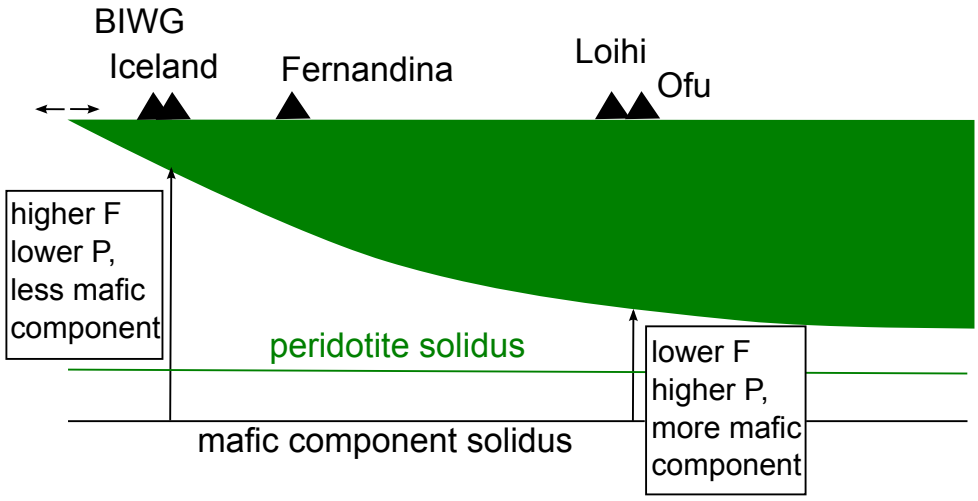

Figure 6: A schematic representation of the effects of LAB thickness on melting pyroxenite/eclogite vs. peridotite. Melts generated at higher pressures (such as melts beneath Ofu and Loihi) will exhibit a pronounced mafic (pyroxenite/eclogite) component and volatile (specifically CO_2 in the source) signature. At shallower pressures, the signature of a mafic component and mantle CO_2 will be diluted owing to a greater proportion of volatile-free peridotite melting. The figure is modified after Prytulak and Elliot (2007) and Dasgupta et al. (2010).

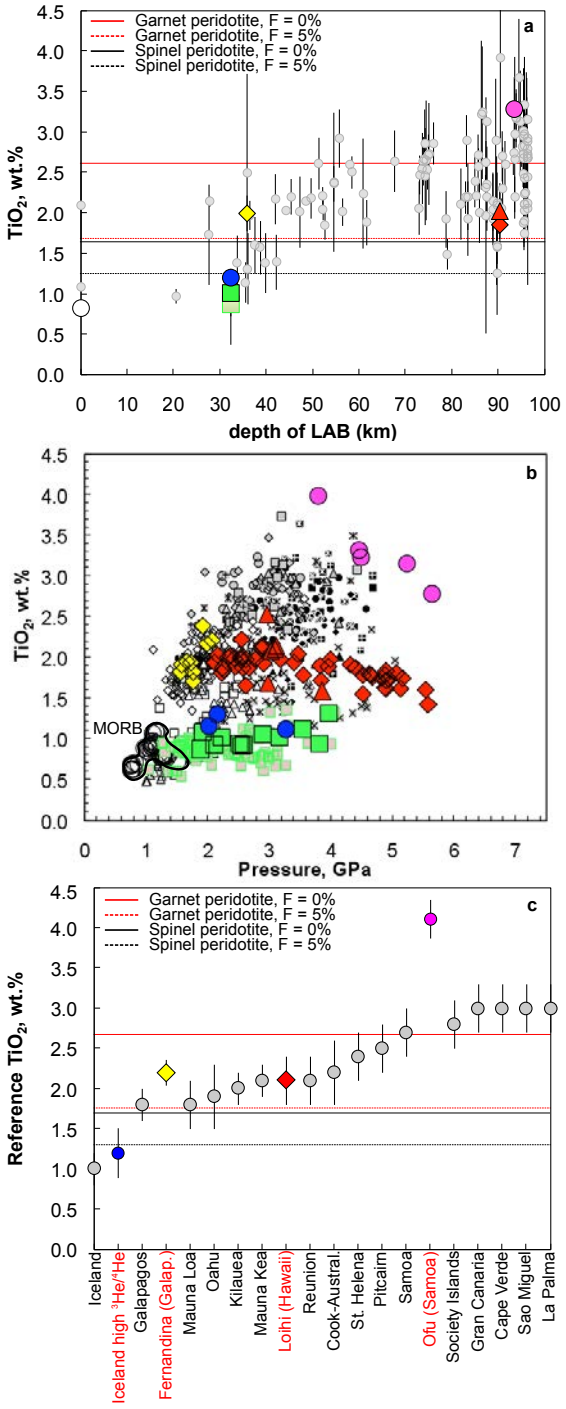

Figure 7

TiO_2 variability in global OIBs and high $^3He/^4He$ lavas. a. Average TiO_2 concentrations are plotted against the depth of the lithosphere-astenosphere boundary (LAB) at the time of volcanism: LAB depths and island-averaged TiO_2 compositions are taken from Dasgupta et al. (2010) (grey symbols). Averages for $^3He/^4He$ localities are calculated in this study. For BIWG, the LAB depth for Iceland is used. The horizontal lines show TiO_2 concentrations that can be obtained by melting of primitive peridotite (McDonough and Sun, 1995) using the Prytulak and Elliot (2007) melt model at the following degrees of melting in the garnet and spinel stability fields: 0% melt (solid lines) and 5% melt (dashed lines), in garnet stability field (red lines) and spinel stability field (black lines). b. A relationship between calculated pressures of melting and concentrations of TiO_2 in global OIBs and high $^3He/^4He$ lavas. The pressures were calculated from major element compositions using the parametrization of Lee et al. (2009), and only lavas with $SiO_2 > 44$ wt.% are shown, as the barometer is not calibrated for highly silica-undersaturated lavas. c. Reference TiO_2 concentration for each of the island groups (all grey symbols) are taken from Prytulak and Elliot (2007). Reference TiO_2 concentrations for high $^3He/^4He$ lavas are calculated using the method outlined for each island group in Prytulak and Elliot (2007). Lines show TiO_2 concentrations are the same as in panel a.

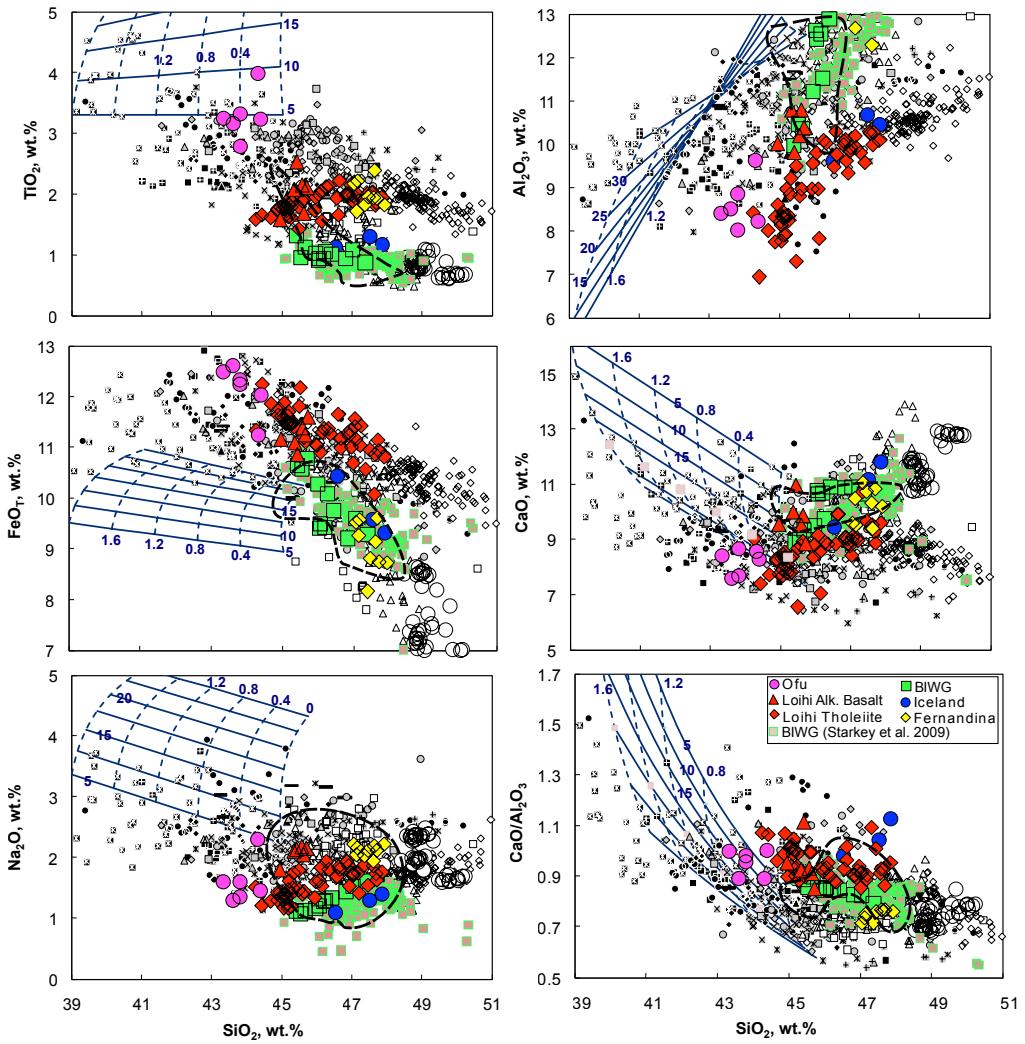

Figure 8

SiO_2 vs. TiO_2, Al_2O_3, FeO_T, CaO, Na_2O and CaO/Al_2O_3 of high $^3He/^4He$ lavas from Baffin Island, Iceland, Fernandina, Loihi (alkalic and tholeiitic lavas) and Ofu. The lavas have been corrected to be in equilibrium with Fo_{88} olivine (the average Mg# of olivines in eclogite-melt hybridization of peridotite according to Mallik and Dasgupta, 2012, 2013, 2014). Also plotted in the figure are fields representing composition of volatile-free peridotite partial melts generated between 2-4 GPa with degree of partial melting up to 20 % (Walter, 1998; Hirose and Kusiro, 1993; Takashi, 1986; Davis et al., 2011) and curves of modeled isopleths of eclogite-melt peridotite hybridization is from Mallik and Dasgupta (2014). The solid and dashed curves are isopleths of eclogite-melt fraction from 0 to 35 wt.% and amount of CO_2 in the eclogite-melt peridotite hybridization (from 0 to 2 wt.%), respectively. The dashed black lines represent dry-peridotite partial melt field. In order to best match the average compositions of the alkalic lavas from Ofu and Loihi with the model,the reacted melt from eclogite-melt hybridization with peridotite has to undergo a second stage mixing with volatile-free peridotite partial melt (see text for details).